

**Kasdi Merbah University Ouargla**

**Faculty of Hydrocarbons, Renewable Energies and Earth and Universe Sciences**

**Renewable Energies Department**



**Memory**

**ACADEMIC MASTER**

**Branch:** Electrotechnics

**Speciality:** Renewable Energy in Electrotechnics

**Presented by:**

Berregui Nabil

Gherier Messaoud

Entitled:

**Modeling. simulation and validation of  
photovoltaic system in southern Algeria**

**Publicly supported**

**on:05/06/2024**

**In front of the jury:**

Z'hour	Abada	Dr	Chairman	Kasdi Merbah University Ouargla
Chouaib	Ammari	Dr	Supervisor	Kasdi Merbah University Ouargla
Hocine	Maammeur	Pr	Examiner	Kasdi Merbah University Ouargla

***Academic year: 2023/2024***

FIRST OF ALL, WE THANK GOD, THE ALMIGHTY, WHO HAS AGREED US IN THIS WORK AND HAS GIVEN US THE STRENGTH TO ACCOMPLISH IT.

WE THANK ALMIGHTY PROFESSOR AMMARI CHOUAIB VERY MUCH FOR HIS GUIDANCE AND VALUABLE AND WISE ADVICE THAT ACCOMPANIED US THROUGHOUT THE TIME OF COMPLETION OF THIS PROJECT.

WE EXTEND OUR SINCERE GREETINGS TO ALL THE MEMBERS OF THE DISCUSSION COMMITTEE.

WE DEDICATE OUR HUMBLE WORK  
IN THE FIRST PLACE TO PARENTS  
WHO HAVE SUPPORTED US  
THROUGHOUT OUR SCHOOL LIFE SO  
THAT THEY MAY FIND OUR  
APPRECIATION AND GRATITUDE.

TO THE TWO GREAT FAMILIES,  
BERREGUI AND GHERIER, TO BE LED  
TO OUR BROTHERS ESPECIALLY, OUR  
FRIENDS IN GENERAL.

TO ALL TEACHERS FROM THE  
ELEMENTARY STAGE SO FAR.

TO OUR BROTHERS IN GAZA AND  
BELOVED PALESTINE, WITH OUR  
CALLING THEM VICTORY.

IN THE END, WE HOPE TO BE OF  
BENEFIT TO OUR MUSLIM NATION.

<b>Acknowledgements</b>	<b>i</b>
<b>Contents</b>	<b>ii</b>
<b>List of Tables</b>	<b>iii</b>
<b>List of Figures</b> .....	<b>iv</b>
<b>Nomenclature</b>	<b>vii</b>
<b>General introduction:</b> .....	<b>1</b>

**CHAPTER I: GENERALITIES ON PHOTOVOLTAICS**

I.1. Introduction .....	2
I.2. solar energy .....	2
I .2.1 Definition.....	2
I.2.2 solar energy in the world and in algeria .....	2
I.3 classification of photovoltaic system .....	4
I.4 Photovoltaic cells .....	5
I.4.1. Photovoltaic cells technologies .....	6
I.4.2. Principle of operation .....	7
I.4.3. Photovoltaic cells characteristics.....	7
I.5 Photovoltaic applications .....	9
I.5.1 In transportation.....	9
I.5.2 In energy generation .....	11
I.5.3 In desalination.....	13
I.5.4 other application .....	16
I.6. Advantages and disadvantages of a PV installation.....	17
I.7. Conclusion.....	18

**CHAPTER II: MODELING OF PHOTOVOLTAIC SYSTEM**

II.1. Introduction.....	19
II.2. Literature review .....	19
II.3. Modeling of PV system .....	24
II.3.1. Modeling of PV .....	24
II.3.2. Comparison between pv model .....	31
II.3.3. Modeling of inverter.....	32
II.3.4. Modeling of the network (the grid) .....	33
II.3.5. Characteristics of the PV model.....	35
II.4. Conclusion .....	35

**CHAPTER III : SIMULATION AND VALIDATION OF PHOTOVOLTAIC SYSTEM**

III.1. Introduction .....	37
III.2. The simulation softwares.....	37
III.3. simulation of PV system models .....	37

III.3.1. Simulation of Standard Model .....	38
III.3.2. Simulation of Simplified Model .....	40
III.3.3. Simulation of Model based on solar irradiation.....	40
III.3.4. Simulation of Seven-parameter Model .....	41
III.3.5. Simulation of Six -parameter Model.....	42
III.3.6. Simulation of Five -parameter Model.....	43
III.3.7. Simulation of Foure -parameter Model.....	44
III.3.8. Simulation of Three -parameter Model.....	45
III.3.9. Simulation of based on technical and meteorological parameters Model .....	46
III.3.10. Comparison between pv model.....	47
III.3.11. simulation of inverter .....	49
III.4. validation of Photovoltaic System models .....	50
III.5. Conclusion .....	53
<b>General conclusion .....</b>	<b>54</b>
<b>References .....</b>	<b>55</b>
<b>Abstract .....</b>	<b>58</b>

## List of Tables

<b>Table( I -1)</b> the advantages and drawbacks of interconnection methods	<b>5</b>
<b>Table (II.1)</b> Electrical characteristics of the PV module Yingli energy (YL250P_29b) in standard test condition	<b>39</b>
<b>Table (III.1)</b> validation of Photovoltaic System models	<b>53</b>

## List of Figures

<b>Figure I- 1:</b> Evolution of cumulative solar thermal electricity capacity (CSP in the world) (2009-2019).....	3
<b>Figure I- 2:</b> Evolution of cumulative solar power capacity (PV and CSP) in the world (2010-2019).....	3
<b>Figure I- 3:</b> Gisement solaire de l'Algérie. ....	4
<b>Figure I- 4:</b> classification of photovoltaic system.....	5
<b>Figure I- 5:</b> Classification of solar PV cells.....	6
<b>Figure I- 6:</b> Principle of operation. ....	7
<b>Figure I- 7:</b> (I-V) and (P-V) characteristics of a PV cell. ....	8
<b>Figure I- 8:</b> The little boat's on solar power.....	9
<b>Figure I- 9:</b> Solar powered car. ....	10
<b>Figure I- 10:</b> Solar electric bikes.....	10
<b>Figure I- 11:</b> Aerial view of the Solarpark Hemau – the solar modules are set up in the open countryside. ....	11
<b>Figure I- 12:</b> Solar shed light. ....	12
<b>Figure I- 13:</b> Categorization of BIPV system. ....	13
<b>Figure I- 14:</b> Membrane distillation.....	14
<b>Figure I- 15:</b> Reverse Osmosis Desalination Plant with Photovoltaic Power Source.....	15
<b>Figure I- 16:</b> (a) Small Open SolWat with reference photovoltaic module (4 h, solar exposure); (b) schematic of the system and use of solar radiation for water disinfection and electricity generation.....	16
<b>Figure II- 1:</b> Comparisons between measured data and calculated data obtained by TSO for single diode model in current-voltage characteristics.....	19
<b>Figure II- 2:</b> Comparisons between experimental data and simulated data obtained by IJAYA for PV module model (a) I-V characteristics; (b) P-V characteristics. ....	20
<b>Figure II- 3:</b> A comparison of I–V curves generated using the extracted parameters from our proposed IADE method (solid line) and the measured data for a multi- crystalline solar module (dots) under different irradiance and temperature conditions. ....	20
<b>Figure II- 4:</b> Comparison between the I–V and P–V characteristics resulted from the experimental data and the double diode model.....	21
<b>Figure II- 5:</b> (a) The double diode model I–V curve and experimental data. (b) The double diode model P–V curve and experimental data.....	21
<b>Figure II- 6:</b> Comparison between experimental data and simulated results for each algorithm: Current-Voltage and Power-Voltage characteristics at $G = 366 \text{ W/m}^2$ , $18 \text{ }^\circ\text{C}$ .....	22
<b>Figure II- 7:</b> Comparison of the experimental and computed I-V and P-V curves of double-diode model for the RTC France solar cell. ....	22
<b>Figure II- 8:</b> The I–V and P–V characteristics prediction by RBFNN based simulations. ....	23
<b>Figure II- 9:</b> Function values versus number of iterations for the tension/compression spring problem.....	23
<b>Figure II- 10:</b> Several examples of simulated I-V curves versus actual I-V curves of the HPCV module at different spectrally corrected direct normal irradiance levels with low cell temperatures. ....	24
<b>Figure II- 11:</b> Ideal electrical circuit of the PV module.....	24
<b>Figure II- 12:</b> Real electrical circuit of the PV module. ....	25
<b>Figure II- 13:</b> Standard Model Scheme. ....	25

<b>Figure II- 14:</b> Simplified Model Scheme.....	27
<b>Figure II- 15:</b> Model based on solar irradiation.....	28
<b>Figure II- 16:</b> Seven-parameter Model Scheme.....	28
<b>Figure II- 17:</b> Six-parameter Model Scheme.....	29
<b>Figure II- 18:</b> Five-parameter Model Scheme.....	29
<b>Figure II- 19:</b> Four -parameter Model Scheme.....	30
<b>Figure II- 20:</b> Three -parameter Model Scheme.....	30
<b>Figure II- 21:</b> Electrical equivalent circuit of the voltage inverter.....	32
<b>Figure II- 22:</b> Scheme of the interface for connecting an inverter to the alternate power grid or to a charge.....	34
<b>Figure II- 23:</b> LC Filter Scheme and RL Load.....	34
<b>Figure III- 1:</b> schema of a current of Standard Model.....	38
<b>Figure III- 2:</b> schema of a photo-current.....	38
<b>Figure III- 3:</b> schema of a saturation current.....	38
<b>Figure III- 4:</b> schema of an inverse saturation current of the diode.....	39
<b>Figure III- 5:</b> I(V) and P(V) characteristics of a standard cell model.....	39
<b>Figure III- 6:</b> schema of a current of Simplified Model.....	40
<b>Figure III- 7:</b> P characteristic of a Simplified cell model.....	40
<b>Figure III- 8:</b> schema of a power of Model based on solar irradiation.....	40
<b>Figure III- 9:</b> P characteristic of a based on solar irradiation cell model.....	41
<b>Figure III- 10:</b> schema of a current of Seven-parameter Model.....	41
<b>Figure III- 11:</b> I(V) and P(V) characteristics of a Seven-parameter cell model.....	42
<b>Figure III- 12:</b> schema of a current of Six -parameter Model.....	42
<b>Figure III- 13:</b> I(V) and P(V) characteristics of a Six-parameter cell model.....	43
<b>Figure III- 14:</b> schema of a current of Five -parameter Model.....	43
<b>Figure III- 15:</b> I(V) and P(V) characteristics of a Five-parameter cell model.....	44
<b>Figure III- 16:</b> schema of a current of Foure -parameter Model.....	44
<b>Figure III- 17:</b> I(V) and P(V) characteristic of a Foure-parameter cell model.....	45
<b>Figure III- 18:</b> schema of a current of Three -parameter Model.....	45
<b>Figure III- 19:</b> I(V) and P(V) characteristic of a Three-parameter cell model.....	46
<b>Figure III- 20:</b> schema of a power of based on technical and meteorological parameters Model.....	46
<b>Figure III- 21:</b> P characteristic of a based on technical and meteorological parameters cell model.....	47
<b>Figure III- 22:</b> Results of the simulation of the nine models of the solar panel 1.....	49
<b>Figure III- 23:</b> Voltage (Va) output signal of the inverter.....	49
<b>Figure III- 24:</b> current (Ia) output signal of the inverter.....	49
<b>Figure III- 25:</b> The simulation of the PV generator station in Matalab.....	50
<b>Figure III- 26 :</b> Results of the simulation of the nine models of el-Hedjira station.....	52
<b>Figure III- 27 :</b> Production at the el-Hedjira station 2023-06-04.....	52



## Nomenclature

Voc	open-circuit voltage
Isc	short-circuit current
FF	fill factor
G	solar irradiation (W/m <sup>2</sup> )
A	cell surface
P <sub>m</sub>	Maximum output power
T <sub>c</sub>	absolute temperature
q	the charge constant of an electron
K	the Boltzmann constant
I <sub>ph</sub>	the current photo
I <sub>S</sub>	the reverse saturation current
Q	is the quality factor
T <sub>r</sub>	Reference temperature K
I <sub>d</sub>	is the current of the diode
R <sub>s</sub>	series resistance
R <sub>p</sub>	parallel resistance shunt
P <sub>pv</sub>	output power
η	panel performance
H <sub>T</sub>	total irradiation
H <sub>b</sub>	direct irradiation
R <sub>b</sub>	direct inclination factor
H <sub>d</sub>	diffused irradiation
R <sub>d</sub>	diffused inclination factor
H <sub>r</sub>	reflecting irradiation
R <sub>r</sub> :	reflected inclination factor
A	photovoltaic panel surface

$I_0$	is the saturation current of the diode
$V_g$	is the energy of the banned band
$K_i$	The current coefficient of the short circuit
$I_{01}, I_{02}$	saturation currents of diode 1 and diode 2.
$\gamma_1, \gamma_2$	the quality factor of diode 1 and diode 2.
$\gamma$	quality factor

### **Abbreviations**

PV	Photovoltaic
CSP	Concentrating Solar Power
GPV	photovoltaic generator
LSHADE	Linearized success history adaptation differential evolution
DE	differential evolution
ABSO	automated balance system optimizer
BBO	biogeography-based optimization
ABC	Artificial Bee Colony
TRR	trust-region reflective
NRO	nuclear reaction optimization
NFi	nuclear fission
Nfu	nuclear fusion
ANN	artificial neuronal network
NOCT	nominal operation cell temperature

### **Greek symbols**

$\eta$	the conversion efficiency
--------	---------------------------

## General introduction

The global electricity consumption has been increasing continuously at the rate of 3% per year; mainly due to the increase of population, techno economic development and the people's needs to create a comfortable life environment[1] On the other hand, over reliance on traditional fossil fuels to provide all energy needs has detrimental effects on the environment, exacerbating climate change, acid rain, air pollution, and global warming. Furthermore, it is anticipated that these conventional resources would run out in the next centuries[2]. As renewable and sustainable energy sources are safe, clean, and environmentally friendly, they should be viewed as promising power generating sources in order to address the environmental and economic issues associated with the production of electricity as well as the aforementioned issues[3]. Solar energy is an endless and clean energy source that provides the Earth with 4000 trillion kWh of insolation per day, among other renewable energy sources[4].

Algeria has several renewable energy resources, the first of which is solar energy of 2,000 hours per year for 6.6KWh PV and 7.5KWh for CSP, and wind energy on Algerian soil of up to 7 and 8 m/s in some southern regions, as well as geothermal energy with more than 240 heat springs and bioenergy resources estimated at 500000 Tep in Algeria[5].

different methodes of modeling the first method is the simplified explicit method which is based on a purely mathematical resolution based on some simplification. The second method is the slope method and which is based partly on its algorithm on a geometric calculation and finally the iterative method that is partly based on its algorithm on numerical resolution[6].

In our study, we aim to search for the results of the best model of the nine different models for the construction of a PV plant in southern algeria.

After a general introduction, the first chapter presents preliminary knowledge of global and local PV energy, in this chapter it presents the evolution of the utilization of light energy and its techniques, characteristics and different applications.

The second Chapter provides a Literature review of the various PV models, modelling of the PV system (the generator and inverter) as well as the Yingli energy properties (YL250P\_29b) used at the el-Hedjira station.

The third and final chapter was to simulating the PV system from the inverter and generator with verification of the system by comparing the results of the simulation with the results of the production from the el-Hedjira station and seeing the best reliable model in southern Algeria.

# CHAPTER I: GENERALITIES ON PHOTOVOLTAICS

## I.1. Introduction

Solar photovoltaic (PV) energy is the most promising of renewable energies, it has many advantages such as being abundant, clean, non-polluting and reliable. It also contributes to reduce CO<sub>2</sub> emissions and protect the environment. In this chapter, we will consider solar energy in the world and Algeria, and then we will talk about the classification of PV systems and their different applications, with an indication of the technologies and properties of the PV cells.

## I.2. solar energy

Solar energy has become a key player in the world's energy future. It is a clean and sustainable source of energy with significant potential for growth in both the world and Algeria.

### I .2.1 Definition

The Sun, a hot gas star, transforms hydrogen atoms into helium through a thermonuclear fusion reaction, causing its surface temperature to reach 5800°K. This energy is converted into radiation in space uniformly and in all directions. The solar constant, a value of 1367 W/m<sup>2</sup>, indicates the solar constant's decrease in extraterrestrial density. Earth receives enough energy from the sun to meet its needs for almost a year, which can be converted into electric energy through photovoltaic panels.

**Solar thermal energy:** This involves generating heat through dark panels or using sun-generated steam to generate electricity.

**Solar photovoltaic energy:** Solar energy, produced directly from light using solar panels, is being utilized in many countries, particularly those lacking conventional energy resources like hydrocarbons or coal[7].

### I.2.2 solar energy in the world and in algeria

The most fundamental points of solar energy in Algeria and the world have evolved over the past few years.

- **in the world**

In terms of solar power generation capacities deployed to date, it is the photovoltaic conversion process (PV) that allows to exploit the light energy from the sun that is very much more important than the one using the thermal component or CSP. (Concentrated Solar Power).

Indeed, although the latter was until the early 2010s the most promising mode for the production of large-scale solar electricity (Project Desertec...) and offered quite attractive possibilities (possibility of storage, connection to the network according to the traditional technical rules...), it has since stagnated. Indeed, its deployment has remained very limited with a cumulative capacity of only 6.2 GW over a decade (2009-2019) and this mainly in Spain and the United States, which are the precursors. At the same time, solar photovoltaics began a remarkable growth in the same period, resulting in a cumulative capacity estimated at 580 GW in 2019. This is due to multiple technical and economic considerations, the most direct of which is the remarkable drop in the costs of the various equipment involved in the photovoltaic installations as well as the relative ease in their deployment. Finally, it is also worth pointing out that the solar reservoir exploitable for a photovoltaic conversion (light spectrum), is more or less present across all regions of the world, hence the notable development of PV even in the northern regions with low sunshine[6].

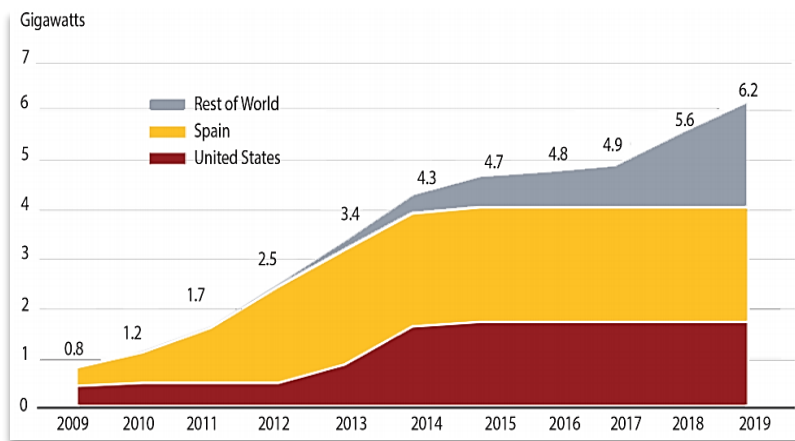


**Figure I- 1: Evolution of cumulative solar thermal electricity capacity (CSP in the world) (2009-2019) [6].**

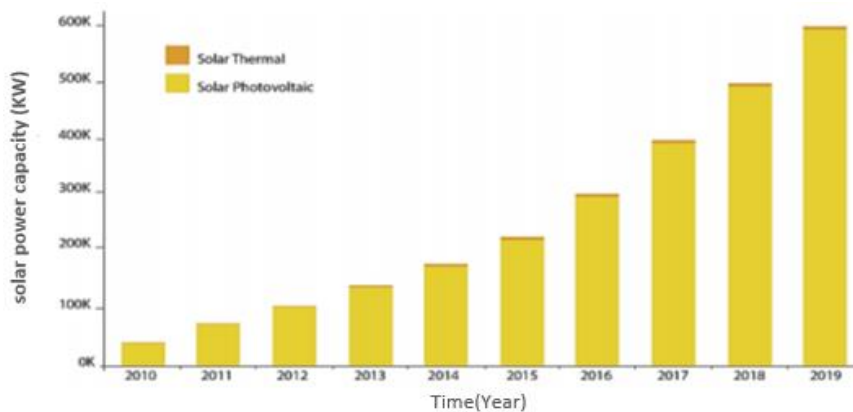
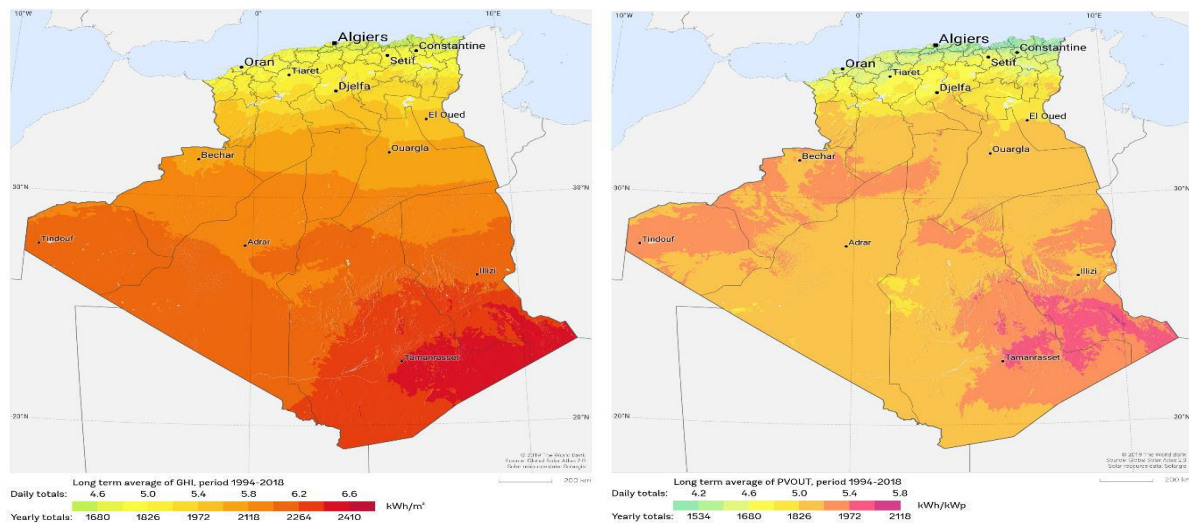


**Figure I- 2: Evolution of cumulative solar power capacity (PV and CSP) in the world (2010-2019) [6].**

- **in Algeria**

Algeria owns one of the world's largest solar reservoirs due to its geographic position. Over 2000 hours of sunlight a year are experienced across nearly the whole country; in the highlands and the Sahara, this number might even approach 3900 hours.

For instance, the total amount of solar energy received daily on a one square meter horizontal surface area varies across the country from 5.1 KWh in the North to 6.6 KWH in the Great South(Figure I -3-a) [6].



(a) Global horizontal irradiation,

(b) Photovoltaic power potential of Algeria

Figure I- 3: Gisement solaire de l'Algérie [8].

As for incident solar radiation from the sun and reaching directly to the earth's surface, without being dispersed through the atmosphere, which remains a basic data for thermal solar concentration (CSP), it can reach 5.5 KWh (Algeria) up to 7.5 KWH (Illizi) per day and per square meter (Figure I -3-b) [6].

### I.3 classification of photovoltaic system

Numerous categorizations have been developed for solar systems; the most commonly applied one is based on three factors: grid connection, integration technique, and features of the photovoltaic system itself.

- **Classification based on power grid connection**

Hybrid systems can be standalone for supply to a remote hamlet or connected to the power grid for mandated worldwide production, depending on the installation goal and capacity.

- **Classification by integrated elements**

Based on integrated elements, hybrid systems are classified into three categories: demand (telecommunication, homes, power grid connection, etc.), storage systems (fuel cell, battery, super capacity, etc.), and generators (solar photovoltaic, etc.). outlined in Table I -1 ( the benefits and disadvantages of connecting techniques).

**Table( I -1) the advantages and drawbacks of interconnection methods.**

Connection methods	Advantages	Drawbacks	Installation Field
DC bus	Reduce loss Simple use	Poor power quality Larger number of converters	Low power application
AC bus	Simple operation Reduce internal loss	Poor power quality Complexity and high cost	Medium and high production
Hybrid bus	Reduce power	Complex control in operating on two different networks	High production

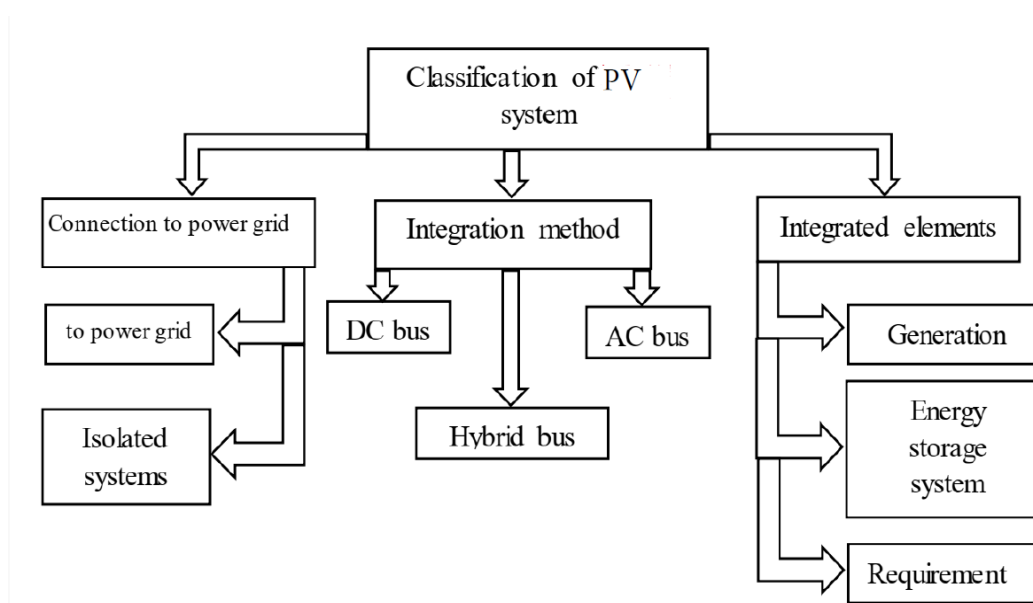


**Figure I- 4: classification of photovoltaic system.**

#### **I.4 Photovoltaic cells**

A photovoltaic cell, or photopile, is the smallest element in a solar system, converting light energy into electric energy. It consists of a thin semiconductor layer, an anti-reflection layer, a conductive grid, and reflective multi-layers. The photovolt effect creates an electromotor force when the cell's surface is exposed to light, generating a voltage ranging from 0.3 V to 0.7 V depending on the material, arrangement, temperature, and ageing of the cell.



### I.4.1. Photovoltaic cells technologies

Owing to their great availability, ease of production, and dependability, silicon-based photovoltaic solar cells are the most commercialized PV cell technology, accounting for 90% of the market share. Nonetheless, other photovoltaic cell technologies are also employed, such as gallium arsenide (AsGa), which exhibits superior electrical energy output compared to silicon. However, because to its high cost and scarcity in the natural world, this kind of material is typically employed in spatial applications. Furthermore, there are other less useful materials as germanium (Ge), selenium (Se), copper indium (CIS), cadmium telluride (CdTe) diselenide, etc. Three primary generations of PV technology may be distinguished (**Figure I-5**), which are listed below:

- First generation photovoltaic cells, which are Silicon based PV cells including monocrystalline and polycrystalline Silicon.
- Second generation photovoltaic cells, including thin-film PV cells such as amorphous (a-Si), copper indium gallium diselenide (CIGS) and cadmium telluride/cadmium sulphide (CdTe/CdS), which aims to use less material whilst preserve the efficiencies of first PV cell generation.
- Third generation photovoltaic cells, including copper zinc tin sulfide (CZTS), a dye-sensitized solar cell (DSSC), organic, perovskite, polymer and quantum dot PV cells, which aims to reach high efficiencies but still use thin film second-generation deposition techniques[8].

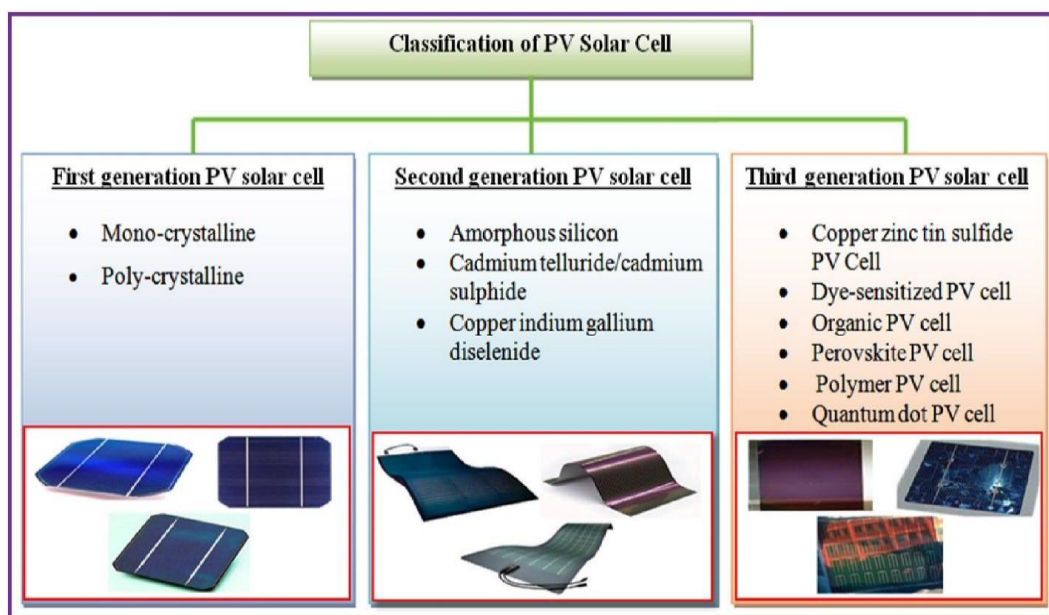


**Figure I- 5: Classification of solar PV cells[8].**

### I.4.2. Principle of operation

When a semiconductor solar cell is exposed to light, it permits electric current to be discharged into an external charge. It functions on the following principle:

The energy photons ( $E_{ph} = h\nu$ ) entering the solar cell transfer their energy to the junction's atoms when the cell is subjected to solar radiation. In semiconductor materials, if the energy is strong enough, it can transfer electrons from the valence band to the conductive band, forming "electron-hole" pairs.

An electrical field that functions as a potential barrier then keeps the electrons (N charges) and the holes (P charges) apart.

When the ends of the cell are charged, the electrons in the N zone join the holes in the P zone through the external connection, creating a potential difference and a circulating electric current. [9]. **(Figure I -6)**

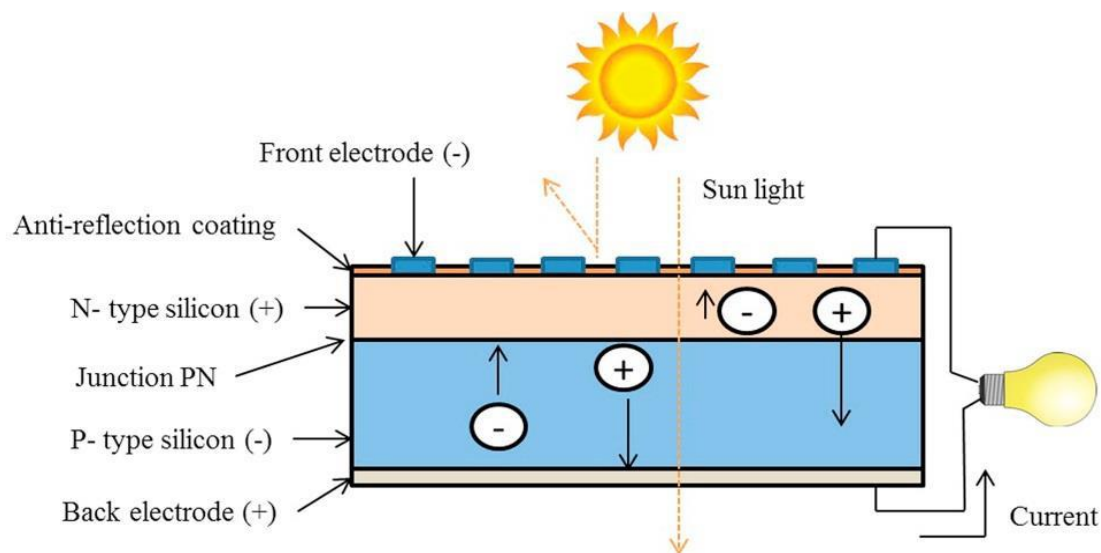


**Figure I- 6: Principle of operation[8].**

The most widespread cells currently are silicon-based (potential difference of 0.6 V) [9].

### I.4.3. Photovoltaic cells characteristics

The basic characteristics of a solar PV cell are the open-circuit voltage ( $V_{oc}$ ), short-circuit current ( $I_{sc}$ ), Maximum output power ( $P_m$ ), the fill factor (FF) and the solar energy conversion efficiency ( $\eta$ ). Photovoltage and photocurrent values at open and short-circuit conditions are known as open-circuit voltage ( $V_{OC}$ ) and short-circuit current ( $I_{SC}$ ), respectively. At short- and open-circuit operation conditions of a PV cell, the output power is equal to zero. **(Figure I -7)** shows schematically the (I-V) and (P-V) characteristic of a PV cell under illumination [8].

- **Short-circuit current ( $I_{sc}$ )**

The short-circuit current ( $I_{sc}$ ) is a very essential parameter of a solar PV cell. It happens in an illuminated, short-circuited PV cell. In this condition ( $V=0$ ).

- **Open-circuit voltage ( $V_{oc}$ )**

The open-circuit voltage ( $V_{oc}$ ) describes the tension between the contacts in no current passing state (open circuit).

- **Maximum power ( $P_m$ )**

The maximum output power ( $P_m$ ) is the greatest possible power value of the PV cell and describes the maximum product of ( $I$  and  $V$ ) values.

$$P_m = I_m \times V_m \quad (1)$$

- **PV cell efficiency ( $\eta$ )**

The conversion efficiency ( $\eta$ ) of a solar PV cell is defined as the ratio between the maximum power ( $P_m$ ) extracted by the PV cell and the product of (solar irradiation ( $G$ ) and PV cell surface ( $A$ )) at which the PV cell is illuminated.

$$\eta = \frac{P_m}{(A \times G)} \quad (2)$$

- **Fill factor (FF)**

The fill factor (FF) is an additional parameter to characterise a PV cell quality; it expresses the ratio by which the ( $I_{sc}$ – $V_{oc}$ ) rectangle is filled by the ( $I_m$ – $V_m$ ) rectangle.

$$FF = \frac{I_m \times V_m}{(I_{sc} \times V_{oc})} \quad (3)$$

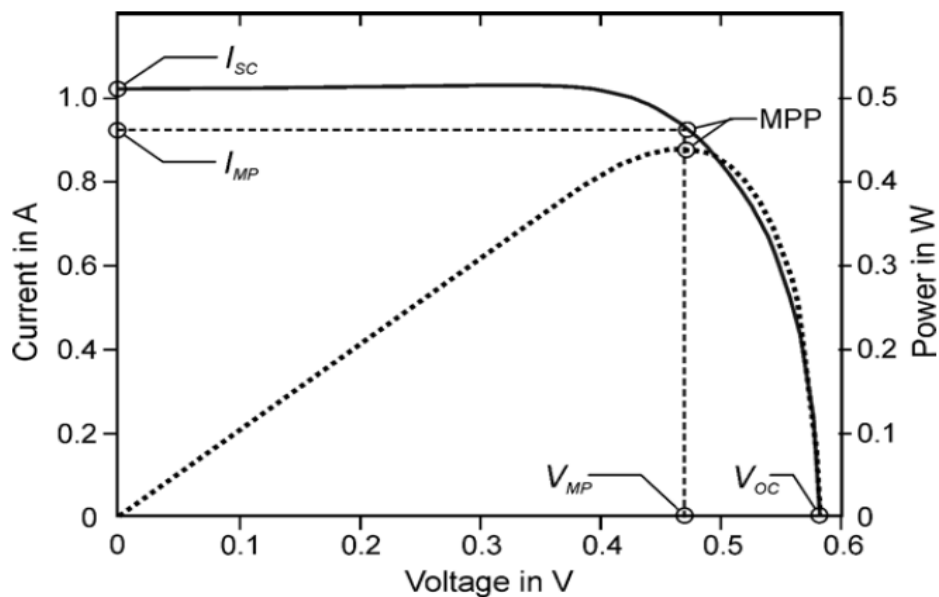


Figure I- 7: (I-V) and (P-V) characteristics of a PV cell [8].

## I.5 Photovoltaic applications

The PV systems are used in several applications, such as transport and power generation. Water dessert and some other applications.

### I.5.1 In transportation

Photovoltaic applications in transportation are the use of solar cells to convert sunlight into electricity for powering vehicles or charging stations.

- **SolarBoat**

Because they are less expensive to purchase, lighter, more portable, easier to operate, and more efficient than their gasoline-powered counterparts, electric outboard motors are also rapidly gaining popularity. Best of all, they are perfect for exploring rural rivers without upsetting the wildlife because they run quietly and don't vibrate.

A 100-watt electric motor will adequately power a modest open boat. Small, lightweight boats can weigh as little as 20 kg (44 pounds) for a 5-meter (15-foot) boat, or as low as 80 kg (175 pounds) for a basic alloy "cabin cruiser." This depends on the material that the boat is made of. For this reason, they don't need a lot of electricity to function well [10].



**Figure I- 8: The little boat's on solar power [30].**

- **Solar car**

Even while the range on solar power might not appear very long, many drivers only take their cars for short trips a few times a week and reside in sunny climates. This might mean that practically all of these people's transportation could be solar-powered. Solar power can be used to increase the range of these cars even in colder regions like the UK and Northern Canada. The batteries can be kept at their ideal temperature by trickle-charging them during the day, which helps to ensure a good range even in cold weather.



A growing number of electric car owners have already converted their vehicles to run on solar power by connecting them to a bigger home solar array, enabling fully green driving over considerably longer distances. In the upcoming year, at least one electric vehicle owners' club plans to provide a solar roof to fit current electric automobiles. Several electric car clubs have created extremely tiny and lightweight solar-powered electric cars and tricycles. [10].



**Figure I- 9: Solar powered car [31].**

- **Solar electric bikes**

To recharge their bike batteries, many owners have constructed a solar array that mounts on the roof of a shed or garage. This comes in particularly handy if you have two battery packs. While the second is being used on the bike, the first may be left charging[10].



**Figure I- 10: Solar electric bikes [32].**

So the PV technology provides a lot of benefits to transport, like...  
Reduction of greenhouse gas emissions: Using a renewable energy source helps reduce

reliance on fossil fuels that contribute to climate change

\_ Enhancing energy security: reducing reliance on traditional sources that can be exposed to price fluctuations or political instability

- Lower fuel costs: solar power can be more cost-effective to run vehicles than fossil fuels.

However, there are also some challenges and constraints, such as:

\_ Low efficiency: The efficiency of converting solar energy into electricity is still relatively limited

\_ High cost: the installation of PV systems is more expensive than conventional techniques.

### **I.5.2 In energy generation**

Photovoltaic applications in energy generation are the use of solar cells to convert sunlight into electricity for various purposes, such as residential, commercial, industrial, or utility-scale power.

- **Solar Power Plants**

in Germany. For instance, an overhead view of the Solarpark Hemau in Regensburg, Bavaria, is seen in (**Figure I-11**). The PV plant has a total capacity of 3,965 kWp, made up of forty partial plants, each with a power of 99.36 kWp [11]



**Figure I- 11: Aerial view of the Solarpark Hemau – the solar modules are set up in the open countryside [11].**

- **Solar shed light**

When purchased as a kit instead than the various parts individually, there are a number of pre-made kits available for installing solar shed lights that frequently give great value for the money.

On the other hand, the producers of these kits frequently claim that their systems will operate at peak efficiency in ideal circumstances. As a result, many individuals are dissatisfied when their "four hours daily usage" in the middle of winter turns out to be closer to twenty minutes[11].



**Figure I- 12: Solar shed light [33].**

- **Building Inegrated Photovoltaic System (BIPV)**

Building-integrated photovoltaics (BIPVs) are solar energy generation devices or systems that are seamlessly integrated into the building envelope and are included in building elements, such as windows, roofs, or facades. This is one of the new strategies aimed at retaining renewable energy in the residential sector. In recent years, BIPV systems—which incorporate PV modules into the building envelope—have grown in favor. Because they enable the production of renewable energy locally and have the potential to replace conventional building components, they lessen the demand for building resources. BIPV systems may screen sunlight while generating supplemental electricity by using shadows, roofs, building breezes, and façade walls. Thin-layer solar panels and bifacial silicon solar panels, two semitransparent PV modules that allow for some light and transparency, are the result of recent advancements in PV technology. Because the BIPV system lets in plenty of natural light, it may be used for clearway applications, windows, and appealing building façades. Therefore, BIPV windows have the benefit of concurrently generating electricity, which lowers the amount of energy needed for lighting and building heating or cooling [12].



**Figure I- 13: Categorization of BIPV system[12].**

So the PV technology provides a lot of benefits to power generation, like...

- \_Reducing emissions of warm gases
- \_Diversifying energy sources.
- \_Supply of electricity in remote or off-grid areas

However, there are also some challenges and constraints, such as:

- \_The first high cost.
- \_The changing nature of solar radiation and non-continuation.
- \_The need to store energy.

### **I.5.3 In desalination**

The scarcity of freshwater resources has emerged as a critical issue in recent decades. Currently, the only nearly inexhaustible source of water is the saline water found in oceans and seas, requiring desalination for usability. Desalination of seawater has become a hopeful solution in regions with limited access to freshwater. However, the high energy consumption, often reliant on fossil fuels, restricts the widespread implementation of desalination systems. In light of global concerns about climate change and the need to reduce greenhouse gas emissions, various studies have explored the potential of supplying the energy required for desalination systems through renewable energy sources[13].



- **Membrane distillation**

The first commercial plant for small amounts of volatile organic compounds (VOCs) removal from contaminated water was developed by Membrane Technology and Research in 1996.

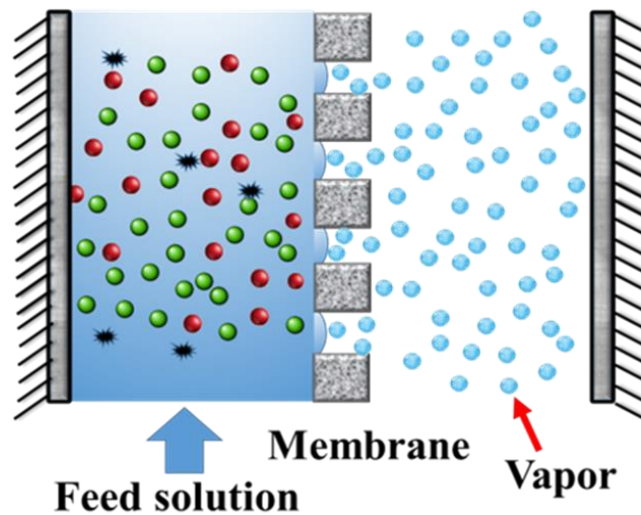


**Figure I- 14: Membrane distillation[34].**

The major applications of PV can be roughly classified into three categories. One is the dehydration of organic solutions; the second is the removal of small amount of organic components from a mixture; the third is the separation of organic mixtures. Among these, the dehydration of organic solutions, in particular, the dehydration of 90–95% ethanol solutions, a difficult separation problem because of the ethanol–water azeotrope at 95% ethanol, remains the most important application in the industry.

Although pevaporation has established itself as one of the most promising technologies for dehydration of organic compounds and separation of organic mixtures in recent years, a stand-alone process may not be economical in industrial applications due to the purity required in production and the limitation of flux[14].

- **Reverse Osmosis Desalination Plant with Photovoltaic Power Source**

Considering that solar systems can only operate during the day, storing photovoltaic electricity allows a reverse osmosis desalination machine to run continuously. Typically, photovoltaic systems are used in combination with batteries to provide electricity throughout the night or during periods of low sunshine intensity. However, the desalination process's operating costs might rise to 17–23 \$/m<sup>3</sup> due to the expensive and limited lifespan of batteries, particularly in hot climates.

The cost of generating one cubic meter of water in photovoltaic-powered reverse osmosis desalination facilities is determined by a number of parameters, such as the recovery ratio, equipment cost, interest rate, and labor cost. Independent photovoltaic-powered reverse osmosis systems for seawater with capacities between 12 and 120 m<sup>3</sup>/day range in price from \$7.95 to \$29 per cubic meter, according to reports. The cost is variable and ranges from \$6.5 to \$9.1 per cubic meter for brackish water with the same capacity. The following elements may be taken into account to lower the expenses associated with the reverse osmosis system's initial capital investment, operation, and maintenance when powered by solar energy [13].



**Figure I- 15: Reverse Osmosis Desalination Plant with Photovoltaic Power Source[35].**

- **New sewage treatment system**

development of the Open solar water treatment (SolWat) system, which is designed for tertiary treatment in a waste water treatment plant (WWTP) and uses only solar energy, since it has the potential to lower energy consumption and increase environmental sustainability. Two prototypes—the Small and Large Open SolWat—of varying sizes have been examined. These included a solar module with an open water disinfection reactor on top of it, and a pumping system that continuously cooled the module's surface with a thin layer of wastewater that fell

freely the energy produced may be utilized to employ renewable energy sources in the future to offset a WWTP's energy needs and self-supply the pumping system [15].

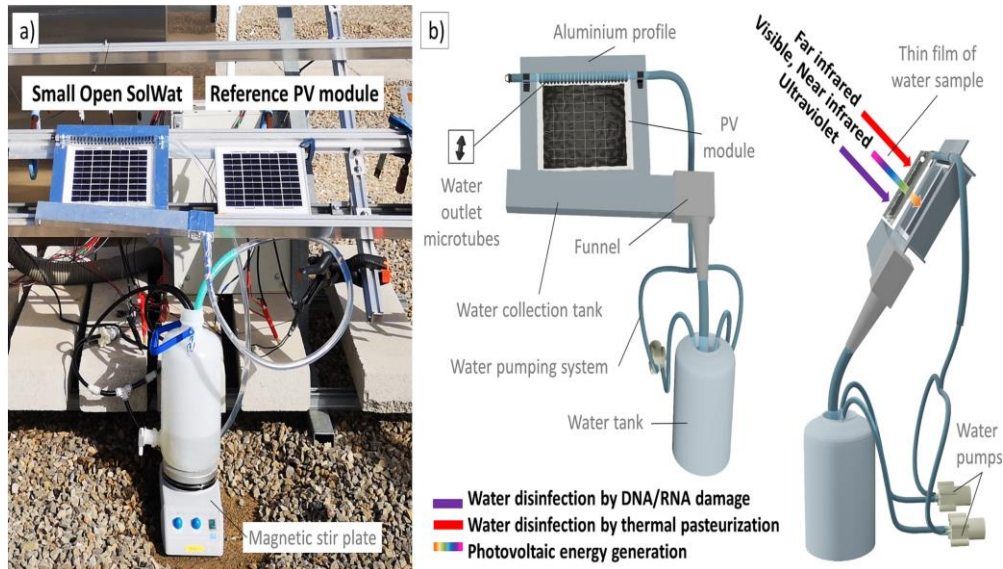


**Figure I- 16: (a) Small Open SolWat with reference photovoltaic module (4 h, solar exposure); (b) schematic of the system and use of solar radiation for water disinfection and electricity generation[15].**

The PV technology provides many benefits for water desalination, like...

- \_Reducing greenhouse gas emissions
- \_Enhancing water security
- \_Water supply is fresh in remote and dry areas

This technology also faces some challenges and constraints, such as:

- \_The first high cost.
- \_Divergence in solar radiation
- \_The need to store energy.

### **I.5.4 other application**

It uses PV in other applications.

- **In hydrogen production**

A significant amount of study has been done in the last several years to look at hydrogen and its energy applications. In order to combat global warming, hydrogen is seen as a very promising stable energy source to replace fossil fuels in the near future. The fact that hydrogen may be created using a variety of energy sources is one of its primary benefits. Specifically, water electrolysis may be utilized to produce hydrogen using photovoltaic (PV) energy[16].

- **in agricultural automation and robotics**

A growing number of agricultural farms are turning to fossil fuels for electricity, but this trend is neither sustainable nor viable in light of climate change concerns and the negative impact fluctuating fossil fuel prices have on production costs. The most plentiful and dependable energy source is solar energy, and the most common electrical renewable method for producing power is photovoltaic (PV) technology. PV technology has big evolved into an economical and energy-saving method in the shift from conventional to modern agriculture. [16].

## **I.6. Advantages and disadvantages of a PV installation**

PV installation offers many advantages

- ✓ The production of this renewable electricity is clean. .
- ✓ Photovoltaic energy is attractive for urban sites, due to their small size, and their silent operation.
- ✓ Since sunlight is available everywhere, photovoltaic energy can be exploited both in mountains in a remote village and in the centre of a large city.
- ✓ Photovoltaic electricity is produced as close as possible to its place of consumption, in a decentralized manner, directly from the user.
- ✓ The materials used (glass, aluminum) are resistant to the worst climatic conditions (including grinding).
- ✓ The lifetime of photovoltaic panels is very long. Some manufacturers offer a 25 year warranty on solar panels.

Unfortunately, there are some disadvantages.

- ☒ Energy production, which depends on sunlight, always variable.
- ☒ The very high cost of power electronics.
- ☒ Low conversion yield.
- ☒ If energy is to be stored with batteries, the cost of the installation increases.
- ☒ Manufacturing pollution.

Despite these disadvantages, the photovoltaic market continues to find applications and to expand. In addition, photovoltaic technology is in a process of maturing in which the disadvantages could lie, especially in terms of manufacturing costs[17].

## **I.7. Conclusion**

In this chapter, we gave a brief overview of PV energy and studied it in Algeria and the world, talking about its main techniques and various, as well as the applications of electric power, without forgetting the disadvantages and advantages of this technology, and the highest electricity increase in the share of electricity production among all renewable energy sources due to the very low prices of PV techniques.

Electrical energy can be used in various applications, including transport, power generation and desalination, as well as in other applications, such as hydrogen production.

CHAPTER II:  
MODELING OF  
PHOTOVOLTAIC  
SYSTEM

## II.1. Introduction

After providing general information about the PV system from its components and some applications in which it is used.

Modelling requires a set of equations that characterize all elements of the system considered.

In this chapter, we're going to review the literature and write the modeling of the system , which includes PV, inverter and the electrical network and a comparison between the PV model.

## II.2. Literature review

A research paper where **Qinzhi Hao and others**[18] introduced a new algorithm to identify the parameters of PV models is an adaptive differential evolution based on the history of multi-strategic success, with a reduction in the size of the linear population (MLSHADE), a combination of Linearized success history adaptation differential evolution (LSHADE) and The covariance matrix adaptation evolution strategy (CAM-ES), where this technique is better presented, but it takes a long accounting time and requires more than 12,000 numbers of job evaluations, which is why MLSHADE's technology is unreliable.

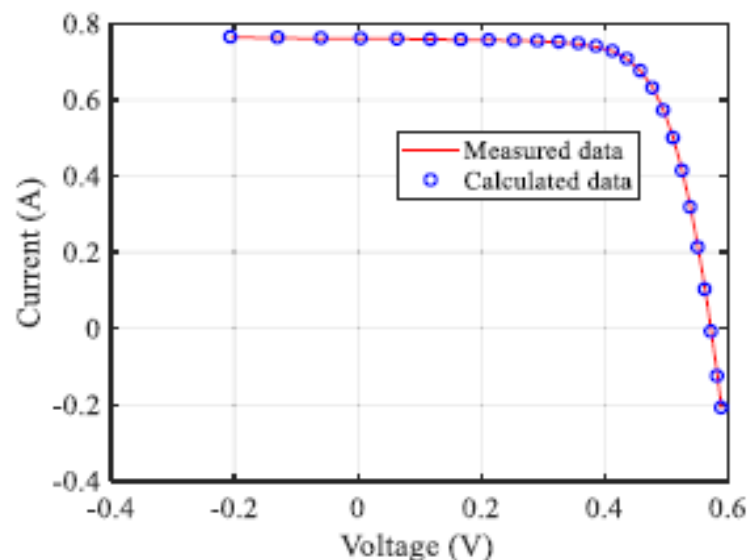


**Figure II- 1: Comparisons between measured data and calculated data obtained by TSO for single diode model in current-voltage characteristics [18].**



**Kunjie Yu and others** [19] proposed the improved JAYA algorithm (IJAYA) to identify the parameters of PV models based on the concept of improving solutions by getting closer to the best and away from the worst. The results showed that the proposed IJAYA has a better and more reliable search accuracy and a faster convergence rate.

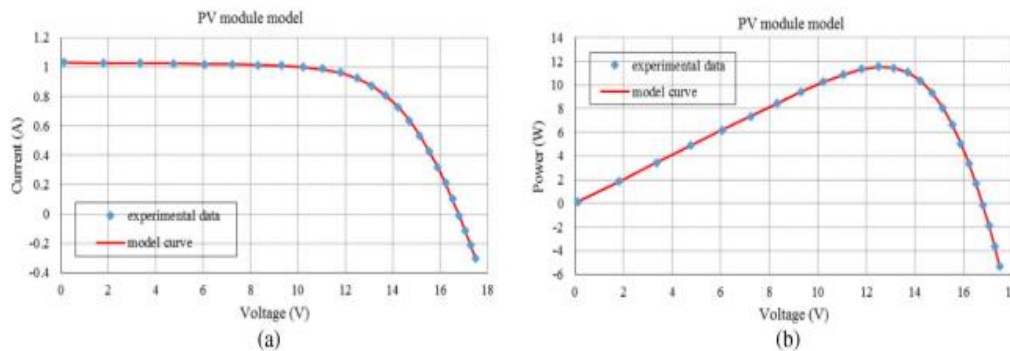


**Figure II- 2: Comparisons between experimental data and simulated data obtained by IJAYA for PV module model (a) I-V characteristics; (b) P-V characteristics[19].**

In this research, **Lian Lian Jiang and others**[20] have proposed an improved way to estimate the parameters of the PV models based on DE (IADE) improved adaptive differential development, using a simple structure based on the feedback of physical fitness in the evolutionary process, and automatically adjusts the two algorithmic control parameters of differential evolution (DE) to include the accuracy of its extractors and also streamlines the process of acceleration and improvement.

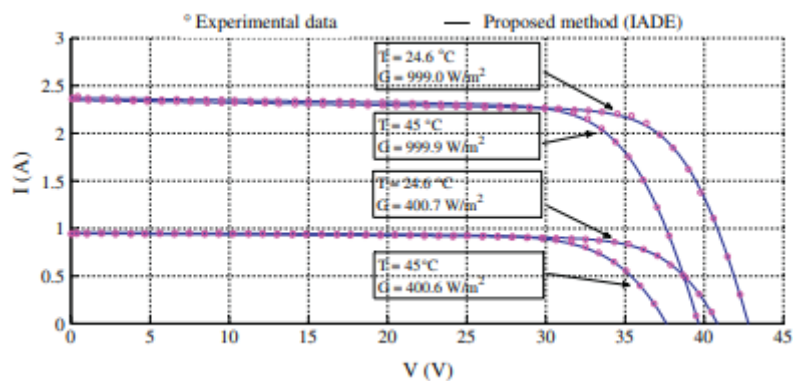


**Figure II- 3: A comparison of I-V curves generated using the extracted parameters from our proposed IADE method (solid line) and the measured data for a multi-crystalline solar module (dots) under different irradiance and temperature conditions[20] .**

In another paper, **Alireza Askaradeh and others**[21] applied automated balance system optimizer (ABSO) to determine the optimal parameters of a commercial silicone solar cell in the diameter of 57 mm (R.T.C. France) The results obtained are better and better suited than those obtained in ways.other



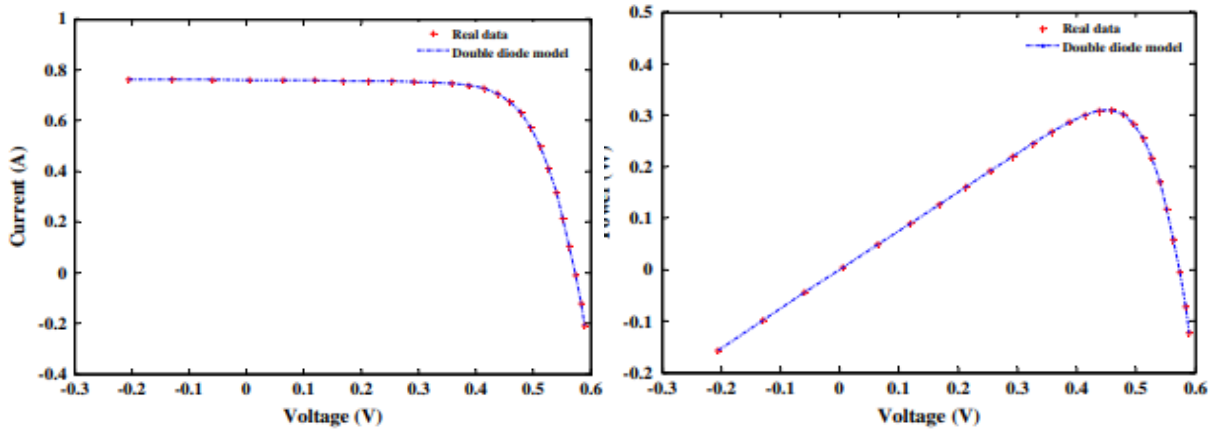


**Figure II- 4: Comparison between the I–V and P–V characteristics resulted from the experimental data and the double diode model [21].**

Qun Niu and others [22] proposed a biogeography-based improvement optimization with Mutation BBO-M used the structure of biogeography-based optimization (BBO). Both the mutation paid for DE's algorithms and the chaos theory are combined into BBO's structure to improve global research. The results show that BBO-M gives a performance similar to the previous results (BBO) and differential evolution DE, Grid-based motion statistics (GMS), Particle Swarm Optimization with Inertia Weight (PSO-W).

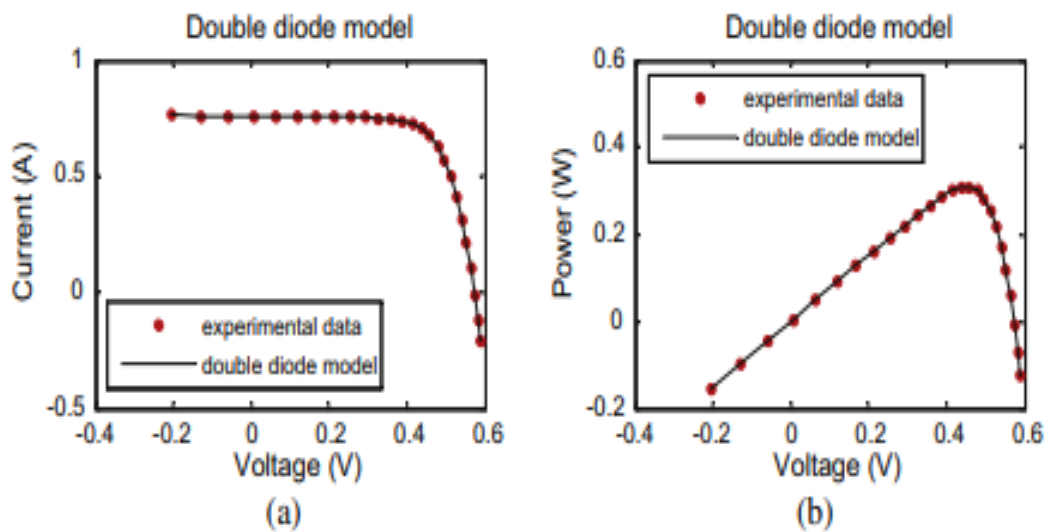


**Figure II- 5: (a) The double diode model I–V curve and experimental data. (b) The double diode model P–V curve and experimental data [22].**

Rabeh Abbasi and others [23] suggested an effective method based on the Salp Swarm (SSA) algorithm for extracting Double-Diode Model (DDM) parameters for electrolytes in order to develop an appropriate objective function where the reliable results and the high accuracy of the SSA-based improver are shown.

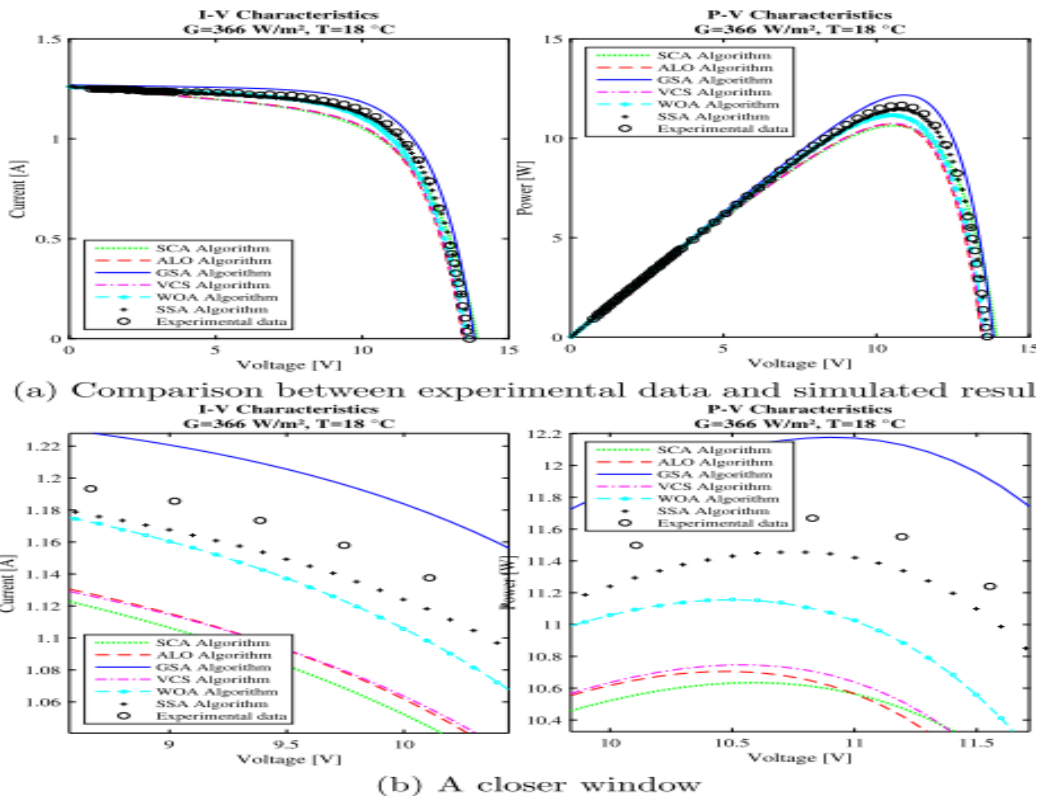


**Figure II- 6: Comparison between experimental data and simulated results for each algorithm: Current-Voltage and Power-Voltage characteristics at  $G = 366 \text{ W/m}^2$ ,  $18 \text{ }^\circ\text{C}$   $T = 18 \text{ }^\circ\text{C}$  [23].**

Lijun Wu and others[24] proposed an algorithm for the improvement of a new ABC-TRR hybrid to improve the recovery of PV models using the I-V curves, which combined the robust global exploration of Artificial Bee Colony (ABC) with the strong local exploitation of trust-region reflective (TRR), and the results showed acceptable accuracy, reliability and a good convergence of 4.69 times compared to the best reported algorithms.

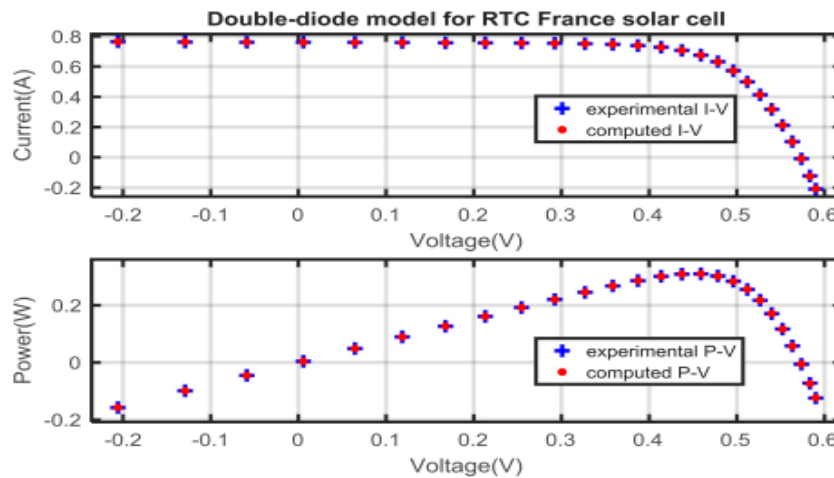


**Figure II- 7: Comparison of the experimental and computed I-V and P-V curves of double-diode model for the RTC France solar cell [24].**

**F Bonanno and others** [25] proposed a new technology based on the neural network of the RBFNN function to emulate complex solar cell properties, which is extremely accurate, but its low computational complexity makes it preferable to model complex and non-linear

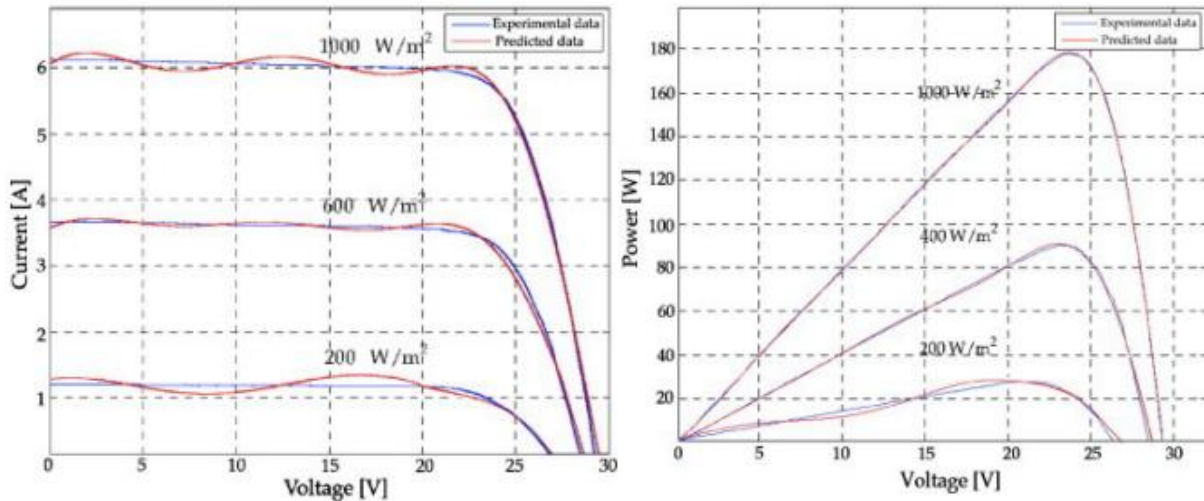


**Figure II- 8: The I–V and P–V characteristics prediction by RBFNN based simulations[25].**

**Zhenglei Wei and others**[26] used a new algorithm inspired by nuclear reaction optimization (NRO) to identify the parameters of the PVCs that include two critical stages of a nuclear fission (NFi) and a nuclear fusion (Nfu) nuclear fusion phase, and Nfu was reported as the best model reported until NRO technology had difficulty getting out of the local ideal situation.

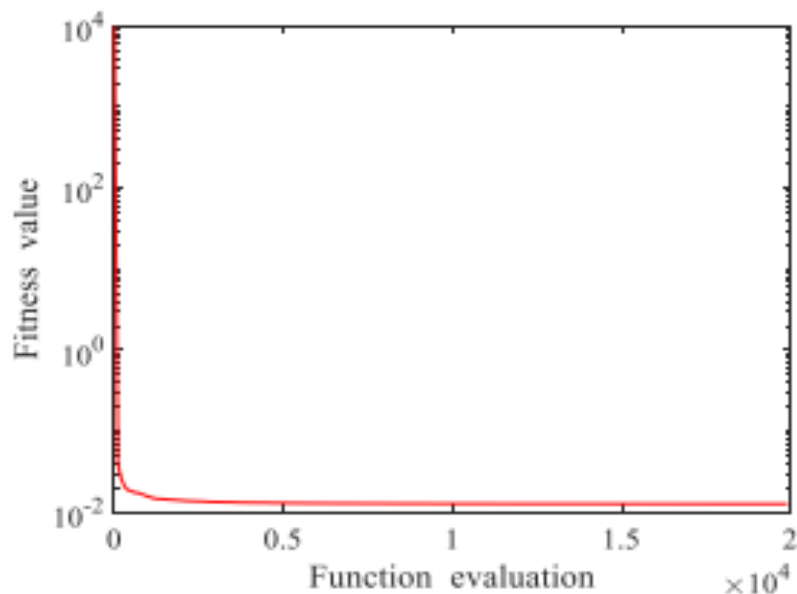


**Figure II- 9: Function values versus number of iterations for the tension/compression spring problem[26].**

**F. Almonacid And others** [27] have introduced a way to simulate the I-V curves of HCPV in any operating situation, depending on different models based on ANN (artificial neuronal network) based on atmospheric parameters and external measurements, so they have the advantage of estimating the electrolytes of HCPV.

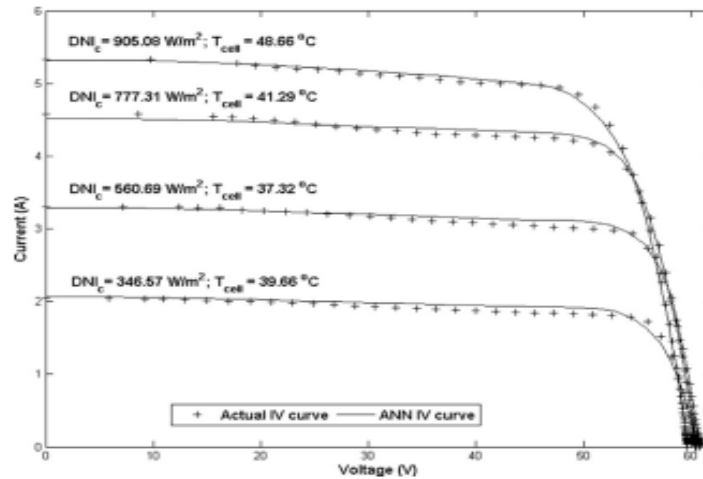


**Figure II- 10: Several examples of simulated I-V curves versus actual I-V curves of the HPCV module at different spectrally corrected direct normal irradiance levels with low cell temperatures [27].**

### II.3. Modeling of PV system

We're going to work in this chapter on modelling and comparing different models of the system as well as modeling the inverter and the electrical grid.

#### II.3.1. Modeling of PV

##### ❖ Ideal electric model

A photovoltaic cell can be described simply as an ideal current source that produces an  $I_{ph}$  current proportional to the incidence light power (Figure II -12), in parallel with a diode that corresponds to the p-n transition area of the PV cell [28].

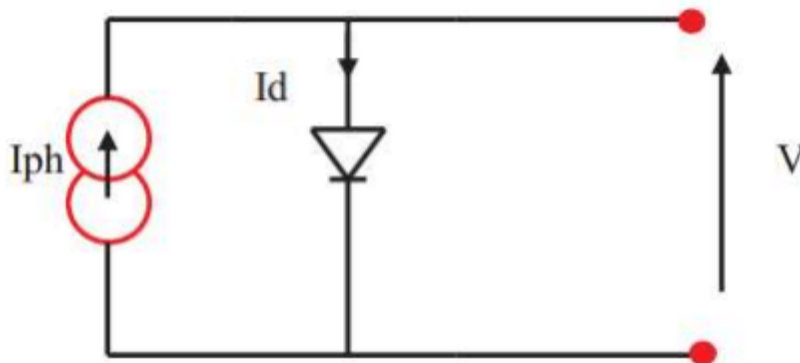


**Figure II- 11: Ideal electrical circuit of the PV module [28].**

$$I = I_{ph} - I_s \left( e^{\frac{qV}{kT}} - 1 \right)$$

❖ **Real electric model**

The previous photovoltaic model did not account for all the phenomena present during the conversion of light energy. Indeed, in the actual case, there is a loss of output voltage as well as leak currents.

So this voltage loss is modeled by a series resistance  $R_s$  and leak currents by a parallel resistance  $R_p$ [28].

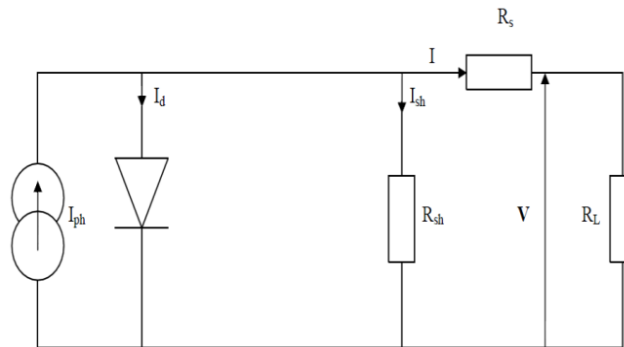


**Figure II- 12: Real electrical circuit of the PV module[28].**

$$I(V) = I_{ph} - I_s \left[ e^{\frac{V + R_s I}{qU_t}} - 1 \right] - \frac{V + R_s I}{R_{sh}}$$

$$U_t = \frac{kT}{q}$$

$\frac{k \cdot T_c}{q}$  : represents the thermodynamic potential;

$T_c$  : absolute temperature;

$q$  : the charge constant of an electron =  $1,602 \cdot 10^{-19}$  C;

$K$  : the Boltzmann constant =  $1.38 \cdot 10^{-23}$ ;

$I_{ph}$  : the current photo;

$I_s$  : the reverse saturation current.

$Q$ : is the quality factor

**A. Standard Model**

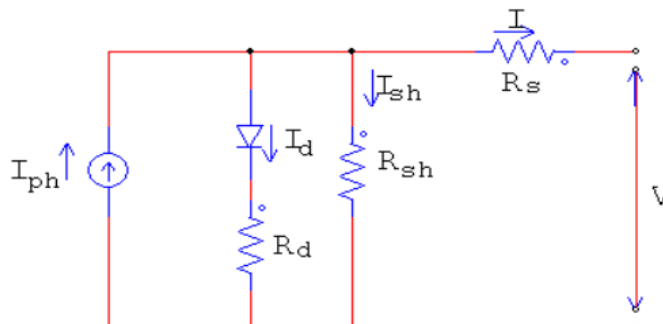


**Figure II- 13: Standard Model Scheme[28].**

By applying the first law of Kirchhoff and neglecting the shunt resistance we write:

$$I = I_{ph} - I_d$$

Or:

$I_{ph}$ : is the photo-current varies with the illumination and temperature, it is determined in relation to values given in the reference conditions:

$$I_{ph} = \left(\frac{G}{G_{ref}}\right) I_{ccref} [1 + K_0(T_c - T_r)]$$

With

G: Clear (W/m<sup>2</sup>).

T<sub>c</sub>: Room temperature (K).

T<sub>r</sub>: Reference temperature (K) = 298.15 = 300

$I_{ccref}$ : Cell short circuit current (module) under standard conditions.

$G_{ref} = 1000 \text{ W/m}^2$  a  $T_r = 25^\circ \text{C} = 298 \text{ K}$

K<sub>0</sub>: Current temperature coefficient.

$I_d$ : is the current of the diode, it is given by:

$$I_d = I_0 \left[ \exp\left(q \frac{V + R_s I}{n k T}\right) - 1 \right]$$

V, I: Voltage (V) and current (A) output from the cell (module).

R<sub>s</sub>: Serial resistance in ohms.

Q: Charge of the electron  $q = 1.602 \cdot 10^{-19}$  coulombs.

K: Constante Boltzmann  $K = 1.381 \cdot 10^{-23}$  J. K. /K.

n: Shape factor, normally between 1 and 2.

$I_0$ : is the saturation current of the diode, given by:

$$I_0 = I_0(T_r) \left(\frac{T}{T_r}\right)^3 \exp\left(\frac{-q V_g}{n k} \left(\frac{1}{T} - \frac{1}{T_r}\right)\right)$$

$$I_0(T_r) = \frac{I_{sc}(T_r) + K_i \Delta T}{\left(\exp\left(\frac{q V_{oc}(T_r)}{n K T_r}\right) - 1\right)}$$

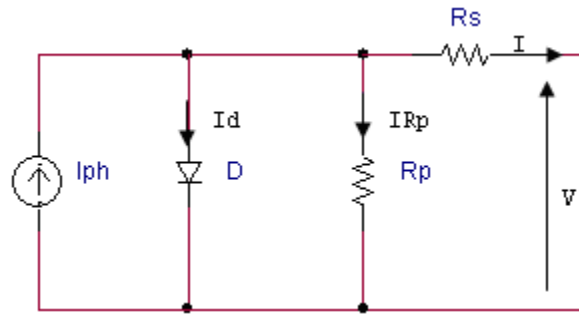
or:  $V_g$  is the energy of the banned band. For sillicium, it is 1.12 eV.

K<sub>i</sub>: The current coefficient of the short circuit, normally provided by the manufacturer.

$\Delta T$ : T-TSTC (in Kelvin, TSTC = 25 °C)

All the constants in the above equations can be determined using data from photovoltaic panel manufacturers and from measured curves  $I = f(V)$ . The global equation for modeling the actual cell (module) is as follows (without considering the shunt resistance) [28]:

$$I = I_{ph} - I_0 \left[ \exp\left(q \frac{V + R_s I}{n K T}\right) - 1 \right]$$

**B. Simplified model:****Figure II- 14: Simplified Model Scheme[28].**

All the constants in the above equations can be determined using data from photovoltaic panel manufacturers and from measured curves  $I = f(V)$ . The global equation for modeling the actual cell (module) is as follows (without considering the shunt resistance) [28]:

$$I_{ref} = I_{sc} \left\{ 1 - C1 \left[ \exp\left(\frac{V_{ref}}{C2V_{oc}}\right) - 1 \right] \right\}$$

With

$$C1 = \left(1 - \frac{I_{mp}}{I_{sc}}\right) \exp\left(\frac{-V_{mp}}{C2V_{oc}}\right) \quad C2 = \frac{\frac{V_{mp}}{V_{oc}} - 1}{1 - \frac{I_{mp}}{I_{sc}}}$$

$I_{sc}$  Short circuit current

$V_{oc}$  Open Circuit Voltage

$I_{mp}$  Current from maximum power point

$V_{mp}$  Maximum power point voltage

The equation (1) can be adapted to other lighting and temperature values according to the following equations:

$$\Delta T = T - T_{ref}$$

$$\Delta I = \alpha \left(\frac{G}{G_{ref}}\right) \Delta T + \left(\frac{G}{G_{ref}} - 1\right) I_{sc}$$

$$\Delta V = -\beta \Delta T - R_s \Delta I$$

$$V_{new} = V_{ref} + \Delta V$$

$$I_{new} = I_{ref} + \Delta I$$

$\alpha$  and  $\beta$  are the current and voltage temperature coefficients respectively

**C. Model based on solar irradiation**

$$P_{pv} = \eta * HT * A = (H_b R_b + H_d R_d + (H_b + H_d) R_r) \eta * A$$

P<sub>pv</sub>: output power

η: panel performance

HT: total irradiation

H<sub>b</sub>: direct irradiation

R<sub>b</sub>: direct inclination factor

H<sub>d</sub>: diffused irradiation

R<sub>d</sub>: diffused inclination factor

H<sub>r</sub>: reflecting irradiation

R<sub>r</sub>: reflected inclination factor

A: photovoltaic panel surface[28].

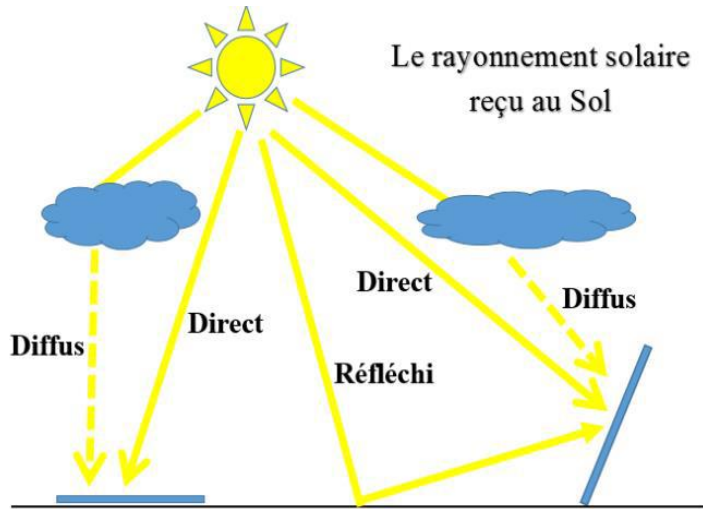


**Figure II- 15: Model based on solar irradiation[28].**

**D. Seven-parameter model(2M7P)**

In any resource the shunt and serial resistance are not negligible, the following scheme represents this model[28]:

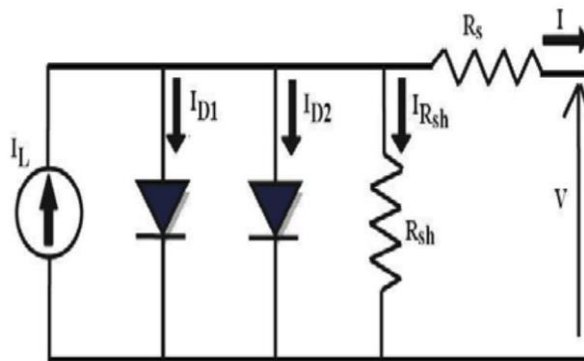


**Figure II- 16:Seven-parameter Model Scheme[28].**

$$I = I_{ph} - I_{D1} - I_{D2} - \frac{V + I.R_s}{R_{sh}}$$

$$I = I_{ph} - [I_{01} (\exp(q \frac{V + I.R_s}{\gamma_1 K T C}) - 1)] - [I_{02} (\exp(q \frac{V + I.R_s}{\gamma_2 K T C}) - 1)] - \frac{V + I.R_s}{R_{sh}}$$

**E. Six-parameter model(2M6P)**

To represent the phenomena of polarization of the junction PN uses this time two diodes. These diodes symbolize the recombination of minority carriers, on the one hand in the surface of materials and on the other in the volume of material[28].



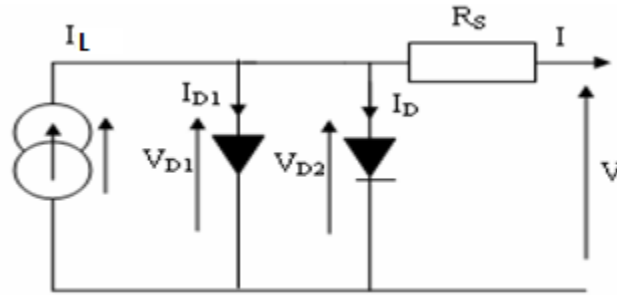


**Figure II- 17: Six-parameter Model Scheme[28].**

The general equation of this model is:

$$I = [I_{ph} - I_{01}(\exp(\frac{q(V+R_s I)}{\gamma_1 K T C}) - 1) - I_{02}(\exp(\frac{q(V+R_s I)}{\gamma_2 K T C}) - 1)]$$

The six parameters are:

$I_{ph}$ : photonic current

$I_{01}$ ,  $I_{02}$ : saturation currents of diode 1 and diode 2.

$\gamma_1$ ,  $\gamma_2$ : the quality factor of diode 1 and diode 2.

$R_s$ : serial resistance

With:

$T_c$ : solar cell temperature .

$K$ ,  $q$ : Boltzmann constant and electron charge constant.

#### **F. Five-parameter model(2M5P)**

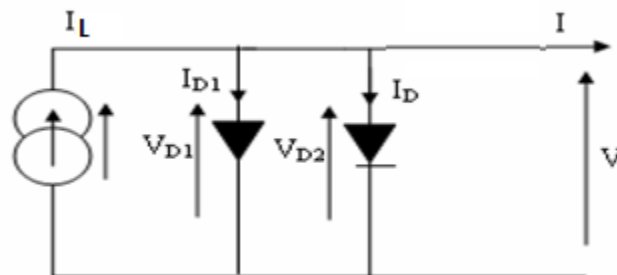


**Figure II- 18: Five-parameter Model Scheme [28].**

$$I = [I_{ph} - I_{01}(\exp(\frac{qv}{\gamma_1 K T C}) - 1) - I_{02}(\exp(\frac{qv}{\gamma_2 K T C}) - 1)]$$

#### **G. Four-parameter model(L4P)**

The four-parameter model (Figure II -20) is a widely used model. This model treats the photovoltaic cell as a power source, dependent on lighting, connected in parallel with a diode and in series with a series resistance  $R_s$ [28].

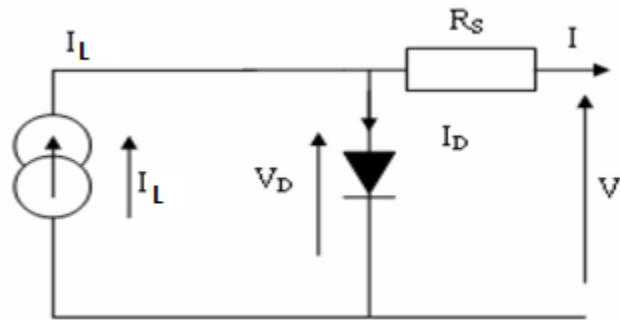


**Figure II- 19: Four -parameter Model Scheme[28].**

The relationship between voltage and current of the photovoltaic generator is given by the following formula:

$$I = I_{ph} - I_0 \left[ \exp \left( \frac{q(V + IR_s)}{\gamma K T_c} \right) - 1 \right]$$

Or :

I, V: current and output voltage of the generator.

$I_{ph}$  and  $I_0$ : represent the photonic current and the reverse saturation current, respectively,

$\gamma$ .  $R_s$ : the quality factor and the serial resistance.

### H. Three-parameter model(L3P)

Assuming the serial resistance ( $R_s$ ) is zero, the four-parameter circuit is reduced to a three-parameter circuit as shown in (Figure II -21). This equivalent circuit is considered ideal[28].

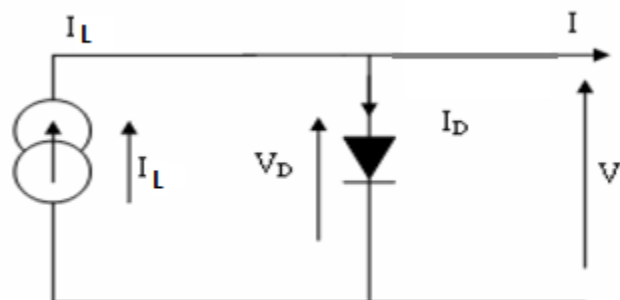


**Figure II- 19: Three -parameter Model Scheme[28].**

The current-voltage ratio of this circuit is:

$$I = I_{ph} - I_0 \left[ \exp \left( \frac{qV}{\gamma K T_c} \right) - 1 \right]$$

The three parameters of this circuit are:

$I_{ph}$  = photonic current

$I_0$  = reverse saturation current

$\gamma$  = quality factor

### Model Choice:

The 4-parameter model is the best model that represents the I(V) characteristics, and the curve returns accurate.

For illumination levels far enough from the reference level, Models that neglect this resistance are used (3P et 5P) [28].

## II. Model based on technical and meteorological parameters

In 2014, Khatib and Elmenreich developed a new technique to calculate the power of a solar photovoltaic system based on six parameters[28]:

- Panel power peak
- Converter performance
- Cable performance
- Temperature coefficient
- Overall irradiation
- Room temperature

$$P_{pv}(t) = [P_{peak} \left( \frac{Gt}{G_{standard}} \right) - \alpha t [T_c(t) - T_{standard}]] \times \eta_{inv} \times \eta_{wire}$$

$$T_c(t) = T_{amb} + \left( \left( \frac{NOCT - 20}{800} \right) \times Gt \right)$$

**NOCT (nominal operation cell temperature):** measurement conditions below 800 W/m<sup>2</sup>, 20°C room temperature and 1m/s wind speed

### Serial Resistance:

$$R_s = \frac{\frac{N_s A K T}{q} \ln \left( 1 - \frac{I_m}{I_{cc}} \right) + V_{co} - V_m}{I_m}$$

## II.3.2. Comparison between pv model

The resulting current I has two exponentials, hence its name. It is also known as 2M7P, where this name specifically specifies the number 7 of parameters to be determined, namely  $I_{ph}, I_{01}, I_{02}, \gamma_1, \gamma_2, R_s$  and  $R_{sh}$

If the shunt resistance is considered infinite, the number of parameters to be determined becomes 6 and the model name in this case is 2M6P. As we also find the 5 parameter model 2M5P where the serial resistance is also not considered.

A simpler description is obtained from the exponential model. This model has one diode less than the two exponential model.

We find a four-type unknown setup that follows:  $I_{ph}$ ,  $I_0$ ,  $\gamma$ ,  $R_s$ , which is called L4P, like an earlier model, a lack of regard for the advantage of chain resistance, which produces a model of three L3P parameters[6].

While the model based on solar irradiation is based on solar radiation, board efficiency and dimensions, the model based on technical and meteorological parameters is based on solar radiation and temperature as well as inverter and cable efficiency.

### II.3.3. Modeling of inverter

The three-phase inverter says two levels is illustrated by its power circuit of the **Figure (II -22)**. On the one hand, we have to distinguish the  $V_{AN}$ ,  $V_{BN}$ ,  $V_{CN}$  branch voltages measured in relation to the negative limit of the continuous voltage  $V_{pv}$ , on the other hand, there are the  $V_{an}$ ,  $V_{bn}$  and  $V_{cn}$  phase voltages Measured with respect to a floating neutral point representing a balanced charge mounted as a star. Composite voltages  $V_{AB}$ ,  $V_{BC}$  and  $V_{CA}$  can be easily extracted from simple voltages[29].

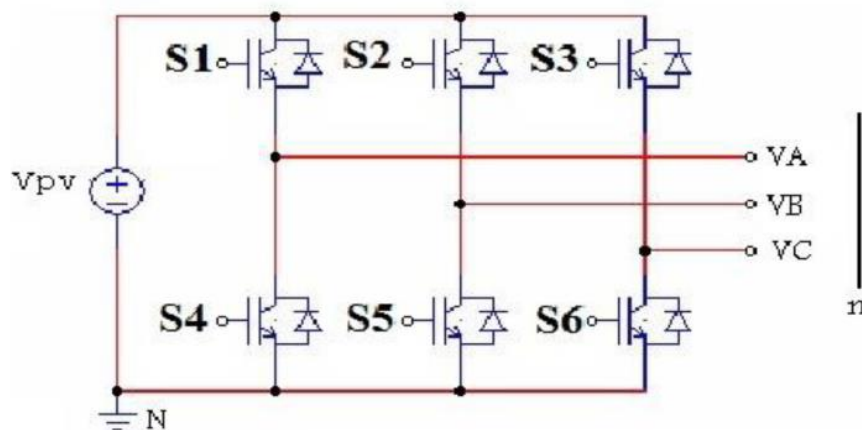


**Figure II- 20: Electrical equivalent circuit of the voltage inverter[29].**

In the power circuit of the three-phase inverter in **Figure (II -22)**, it should be noted that the states of the switches of the same arm are complementary. Using these switch states, we

can obtain the output branch voltage of the inverter measured relative to the negative border of the continuous side voltage as follows:

$$\begin{aligned} V_{AN} &= S1. VPV \\ V_{BN} &= S2. VPV \\ V_{CN} &= S3. VPV \end{aligned} \quad (1)$$

Either S1, S2 and S3 denote the states of the phase switches A, B and C, respectively.

$$\begin{aligned} V_{AB} &= V_{AN} + V_{NB} = V_{AN} - V_{BN} = (S1 - S2)VPV \\ V_{BC} &= V_{BN} + V_{NC} = V_{BN} - V_{CN} = (S2 - S3)VPV \\ V_{CA} &= V_{CN} + V_{NA} = V_{CN} - V_{AN} = (S3 - S1)VPV \end{aligned} \quad (2)$$

- **Composite tensions are**

$$\begin{bmatrix} V_{AB} \\ V_{BC} \\ V_{CA} \end{bmatrix} = \begin{bmatrix} 1 & -1 & 0 \\ 0 & 1 & -1 \\ -1 & 0 & 1 \end{bmatrix} \begin{bmatrix} S1 \\ S2 \\ S3 \end{bmatrix} VPV \quad (3)$$

We can write the equation (20) in matrix form

$$\begin{aligned} V_{an} &= \frac{2}{3}V_{AN} + \frac{1}{3}(V_{BN} + V_{CN}) \\ V_{bn} &= \frac{2}{3}V_{BN} + \frac{1}{3}(V_{AN} + V_{CN}) \\ V_{cn} &= \frac{2}{3}V_{CN} + \frac{1}{3}(V_{BN} + V_{AN}) \end{aligned} \quad (4)$$

- **The simple tensions are**

$$\begin{bmatrix} V_{an} \\ V_{bn} \\ V_{cn} \end{bmatrix} = \frac{VPV}{3} \begin{bmatrix} 2 & -1 & -1 \\ -1 & 2 & -1 \\ -1 & -1 & 2 \end{bmatrix} \begin{bmatrix} S1 \\ S2 \\ S3 \end{bmatrix} \quad (5)$$

#### II.3.4. Modeling of the network (the grid)

Charges are the consuming elements of electrical power in a system. The consumption of this electrical power depends on the characteristics of the charge. Correct modeling of these characteristics is essential to fine represent the behavior of the load. **Figure (II -23)** shows the model of the charge connected to the voltage inverter[29]:

- LC filter
- balanced charges of nature RL
- power grid base voltage

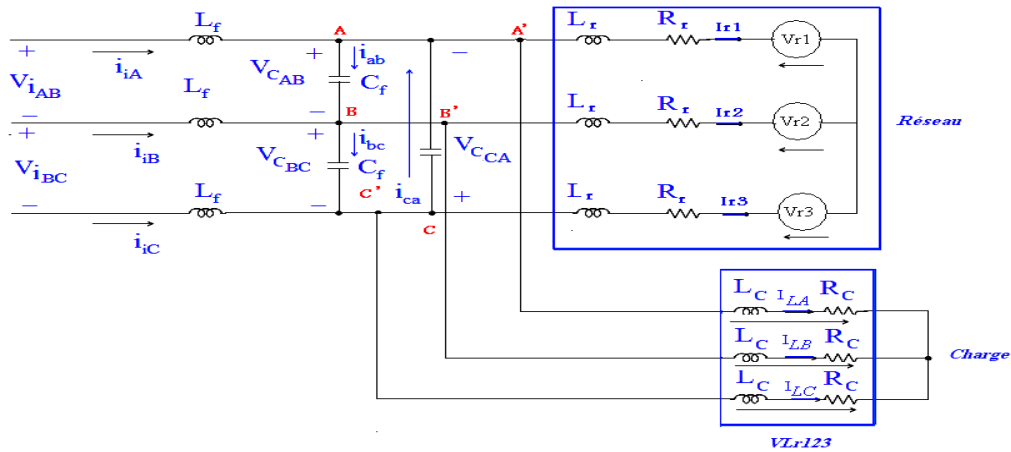


**Figure II- 21: Scheme of the interface for connecting an inverter to the alternate power grid or to a charge [29].**

Electricity distribution network. It is based on a three-phase system of tensions. It can generally be considered that  $(V_a V_b V_c)$  is a direct balanced three-phase voltage system. The same applies to  $(U_{ab} U_{bc} U_{ac})$ .

$$V_a = V_m \sin(\omega t)$$

$$U_{ab} = V_a + V_b$$

$$V_b = V_m \sin(\omega t - \frac{2\pi}{3}) \tag{6}$$

$$U_{bc} = V_b + V_c \tag{7}$$

$$V_c = V_m \sin(\omega t - \frac{4\pi}{3})$$

$$U_{ca} = V_c + V_a$$

$$V_m = \sqrt{2} V_{eff}$$

$$U_m = \sqrt{3} V_m \tag{8}$$

$$U_{eff} = \sqrt{3} V_{eff}$$

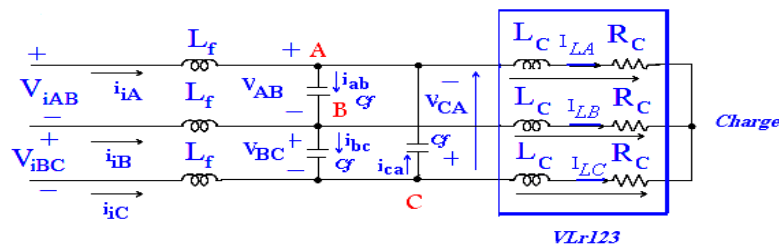


**Figure II- 22: LC Filter Scheme and RL Load[29].**

By applying Kirchhoff's law to nodes A, B, and C, the current and voltage equations of the LC filter described in **Figure (II -24)** are given as follows[29]:

- Nodes (A):

$$iia+ica=iAB+iLA \rightarrow iia+Cf\frac{dvca}{dt} = Cf\frac{dvab}{dt} + iLA \quad (9)$$

- Nodes (B):

$$iiB+iBC=iBC+iLB \rightarrow iiB+Cf\frac{dvab}{dt} = Cf\frac{dvca}{dt} + iLB \quad (10)$$

- Nodes ©:

$$iiC+iBC=iCA+iLC \rightarrow iiC+Cf\frac{dvbc}{dt} = Cf\frac{dvca}{dt} + iC \quad (11)$$

### II.3.5. Characteristics of the PV model

In this work, we simulated the Yingli energy (YL250P\_29b) photovoltaic module that includes 60cells 156\*156mm multicrystalline silicon solar cells connected in series.

The Yingli energy (YL250P\_29b)PV module can produce a maximum power of 250 watts at 29.8 volts. This allowed us to determine the power based on voltage and current based on the voltage of the module studied for a lighting of 1000 W/m<sup>2</sup>.

The electrical characteristics of the Yingli energy (YL250P\_29b) photovoltaic module under standard test conditions are shown in the **(table II.1)**.

**Table (II.1): Electrical characteristics of the PV module Yingli energy (YL250P\_29b) in standard test condition.**

Size	Value
- Clearly standard, E.	1000 W/m <sup>2</sup>
- Standard temperature, T.	25 C
- Maximum peak power, P <sub>m</sub> .	250 W
- Optimum voltage, V <sub>opt</sub> .	29.8 V
- Optimum current, I <sub>opt</sub> .	8.39 A
- Open circuit voltage, V <sub>oc</sub>	37.6 V
- Short circuit current, I <sub>cc</sub>	8.92 A

### II.4. Conclusion

We have modeled each of the components of the entire PV system based on previous literature models (the PV model, inverter and the network). This is a fundamental step that allows us to present a certain number of models and then assess the characteristics of each



element of the installation as well as the parameters of the component in the PV systems. We're always looking to work near MPP's maximum power point to make good use of the system.

**CHAPTER III :**  
**SIMULATION AND**  
**VALIDATION OF**  
**PHOTOVOLTAIC**  
**SYSTEM**

### III.1. Introduction

In this chapter, we simulated all the equipment that represents the PV system in Matalab/Simulink environment, like the PV generator with its nine different models. The results obtained will compared with the results presented by this system in el-Hedjira station in southern Algeria

### III.2. The simulation softwares

There are many software programs available to simulate photovoltaic solar systems, such as Homer Pro and PVsyst, which are common simulation and design programs for solar solar systems. Moreover, Matlab is a powerful programming environment that offers many opportunities to study and study these systems.

**Homer Pro:** Its graphical interface is easy to use, making it an ideal choice for beginners. It also offers many benefits for studying the viability of solar energy projects, such as cost and risk analysis.

**PVsyst:** A more advanced program than Homer Pro, offering more advantages for modeling and simulation of photovoltaic solar panels.

**Matlab** is not a program specific to photovoltaic solar systems, but it provides a robust and flexible programming environment for studying and studying these photovolt systems. It is distinguished by the creation of models for solar photovoltaic systems by taking into account all the necessary information and by offering high accuracy in calculations. This allows precise simulation of the behavior of photovoltaic solar systems and also provides many analytical tools for solar photovolt data, Like statistical analysis and signal processing. Matlab is therefore a powerful tool for studying and evaluating photovoltaic solar systems, but requires technical expertise and knowledge of the software. Although Homer Pro and PVsyst are more user-friendly programs for beginners.

### III.3. simulation of PV system models

Simulation of 9 different models of Yingli energy (YL250P\_29b) to display V\_I properties and V\_P properties, as well as a simulation of the inverter for use in the conversion from DC to AC, enabling us to integrate it with the charge.

III.3.1. Simulation of Standard Model

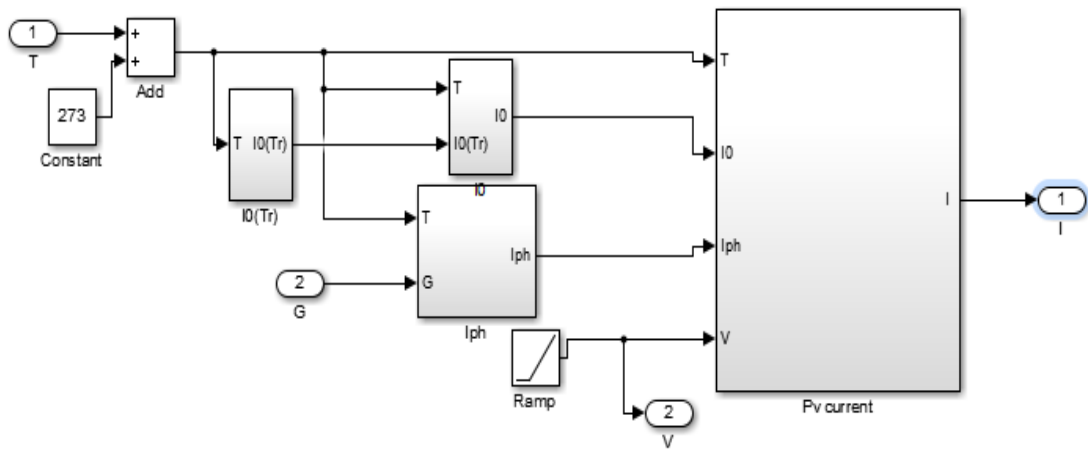


Figure III- 1: schema of a current of Standard Model.

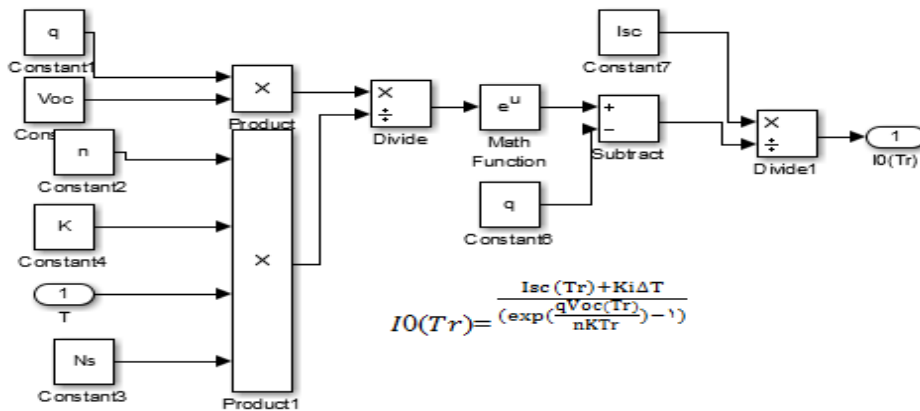


Figure III- 2: schema of a photo-current.

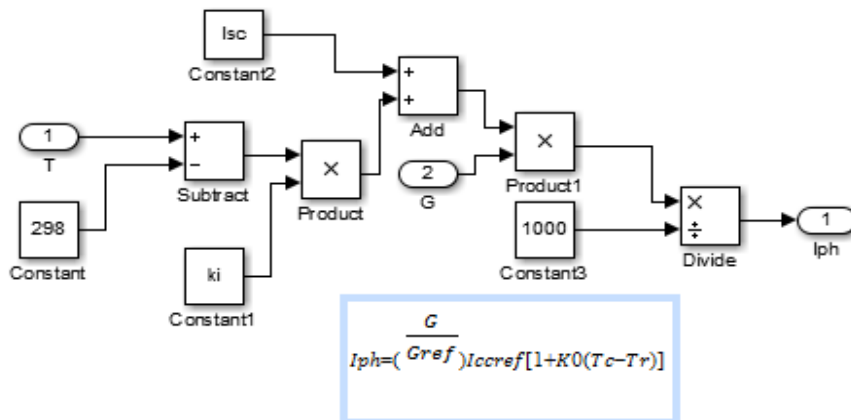
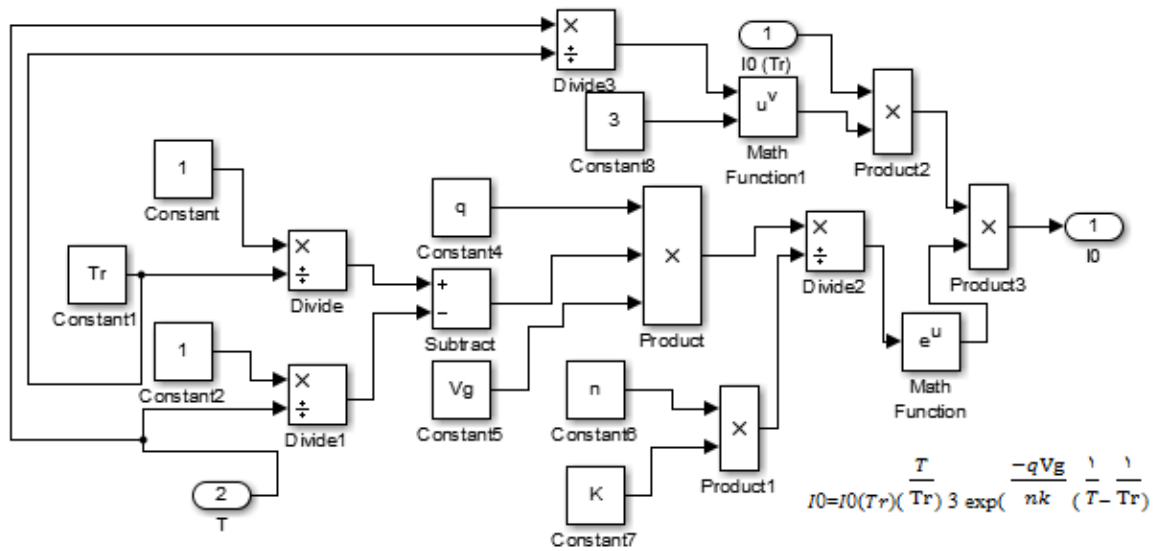
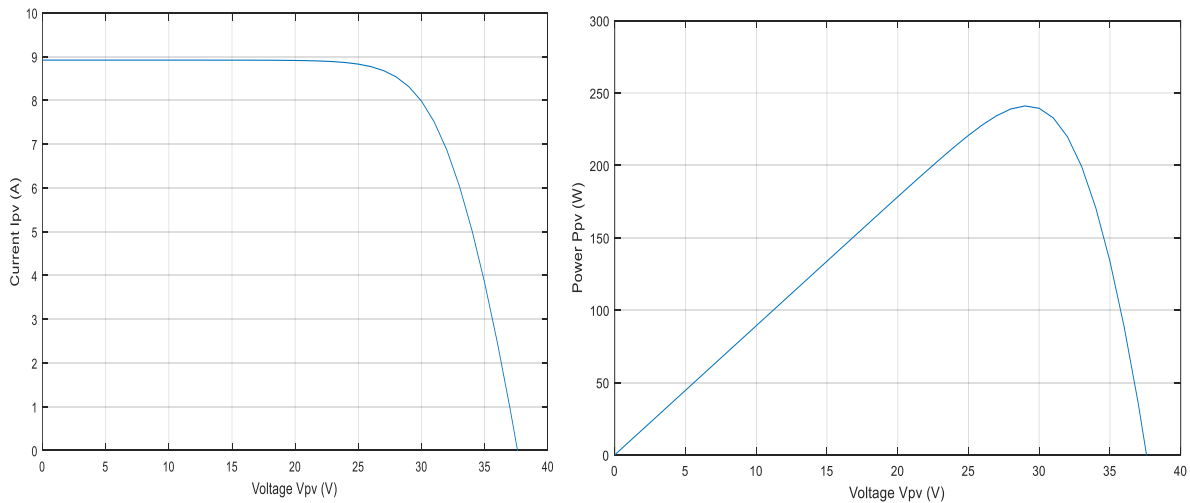


Figure III- 3: schema of a saturation current.



**Figure III- 4: schema of an inverse saturation current of the diode.**

The results obtained from the simulation (programming using the MATLAB software) of a characteristics current-voltage I(V) and power-voltage P (V) of the photovoltaic cell in standard conditions (T = 25°C. E = 1000 W / m<sup>2</sup>) are represented in the following figure: The following figure represents the current characteristic - voltage of a standard solar cell model in conditions of E = 1000W / m<sup>2</sup> and T = 25°C.



**Figure III- 5: I(V) and P(V) characteristics of a standard cell model.**

The characteristic power-voltage of a solar cell in conditions of E=1000 W/m<sup>2</sup> and T=25°C. The maximum power is P max = 240W. It is noted that, when the voltage increases the power increases until it reaches the optimal value (P max) then it decreases.

**III.3.2. Simulation of Simplified Model**

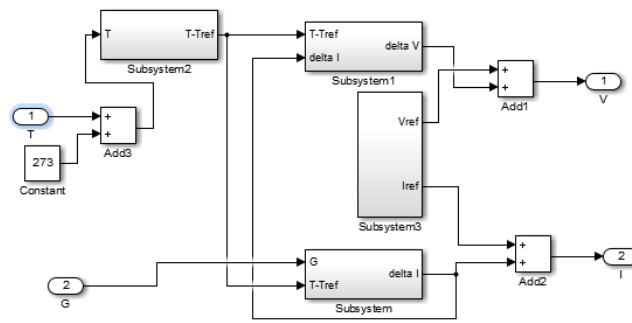


**Figure III- 6: schema of a current of Simplified Model.**

The results obtained from the simulation (MATLAB programming) of P energy properties of the PV are a Simplified model in conditions for solar radiation and heat on 04-06-2023 from 6 a.m. to 20 p.m In the new el hadjira touggourt. in the following form: The following figure represents energy characteristic of the Simplified solar cell model. The maximum power is  $P_{max}=225W$ . It is noted that, when time increases power increases until it reaches the optimal value ( $P_{max}$ ) then it decreases. With an observation of a device malfunction at 15.30 p.m.

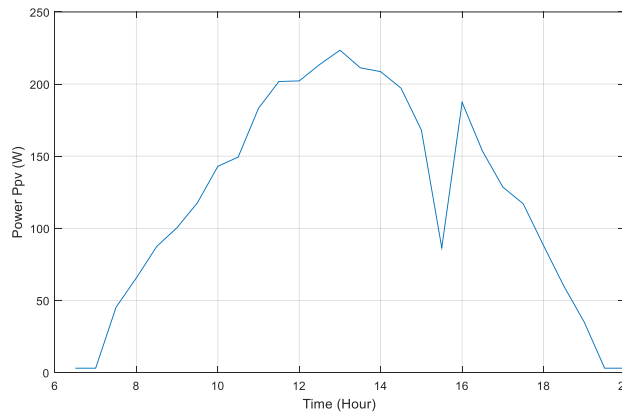


**Figure III- 7: P characteristic of a Simplified cell model.**

**III.3.3. Simulation of Model based on solar irradiation**

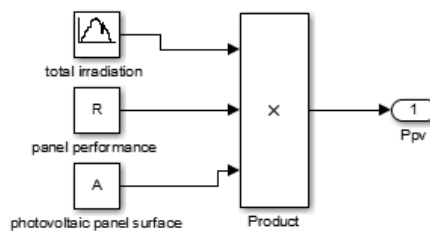


**Figure III- 8: schema of a power of Model based on solar irradiation.**

The results obtained from the simulation (MATLAB programming) of P energy properties of the PV are based on solar irradiation model in conditions for solar radiation on 04-06-2023 from 6 a.m. to 20 p.m. In the new el "hadjira touggourt" . in the following form: The following figure represents energy characteristic of the Simplified solar cell model. The maximum power is  $P_{max}=254W$ . It is noted that, when time increases power increases until it reaches the optimal value ( $P_{max}$ ) then it decreases. With an observation of a device malfunction at 15.30 p.m.

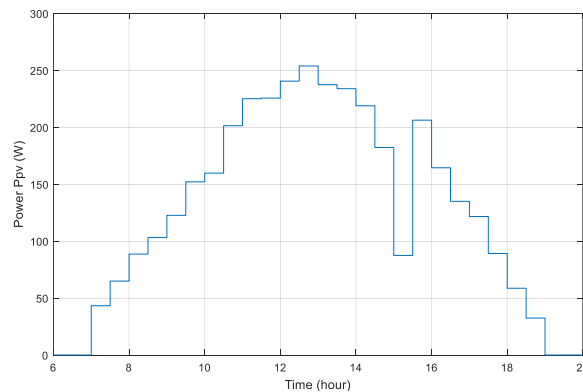


**Figure III- 9: P characteristic of a based on solar irradiation cell model.**

### III.3.4. Simulation of Seven-parameter Model

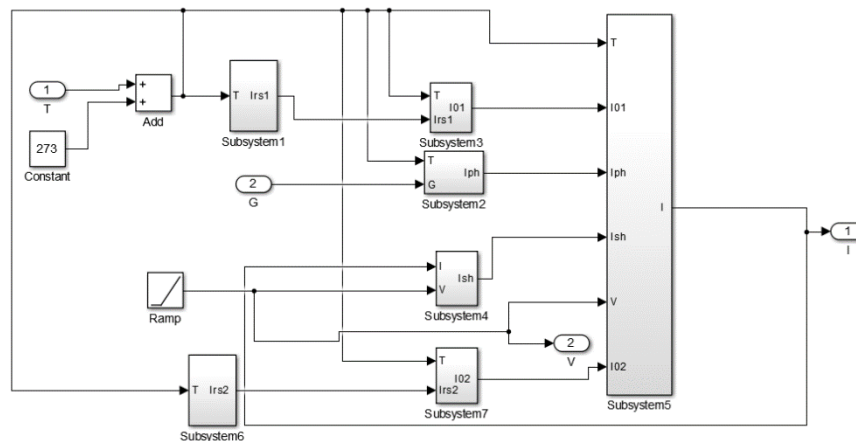


**Figure III- 10: schema of a current of Seven-parameter Model.**

The results obtained from the simulation (programming using the MATLAB software) of a current characteristics -voltage  $I(V)$  and power-voltage  $P(V)$  of the photovoltaic cell in Seven-parameter conditions ( $T = 25^{\circ}C$ ,  $E = 1000 W / m^2$ ) are represented in the following figure:

The following figure represents the current characteristic - voltage of a standard solar cell model in conditions of  $E = 1000W / m^2$  and  $T = 25^{\circ}C$ .



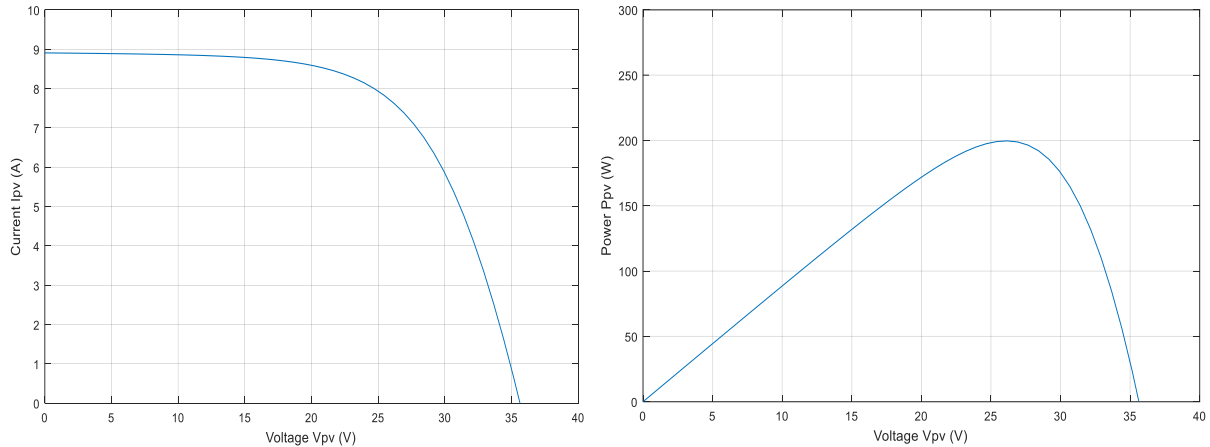


**Figure III- 11: I(V) and P(V) characteristics of a Seven-parameter cell model.**

The characteristic power-voltage of a solar cell in conditions of  $E=1000 \text{ W/m}^2$  and  $T=25^\circ\text{C}$ . The maximum power is  $P_{\text{max}} = 200\text{W}$ . It is noted that, when the voltage increases the power increases until it reaches the optimal value ( $P_{\text{max}}$ ) then it decreases.

**III.3.5. Simulation of Six -parameter Model**

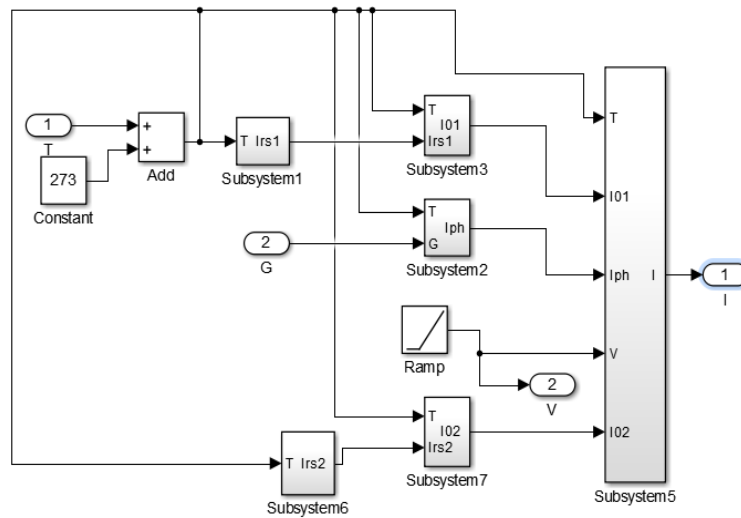


**Figure III- 12: schema of a current of Six -parameter Model.**

The results obtained from the simulation (programming using the MATLAB software) of a current characteristics -voltage I(V) and power-voltage P (V) of the photovoltaic cell In Six-parameter conditions ( $T = 25^\circ\text{C}$ .  $E = 1000 \text{ W} / \text{m}^2$ ) are represented in the following figure: The following figure represents the current characteristic - voltage of a standard solar cell model in conditions of  $E = 1000\text{W} / \text{m}^2$  and  $T = 25^\circ\text{C}$ .

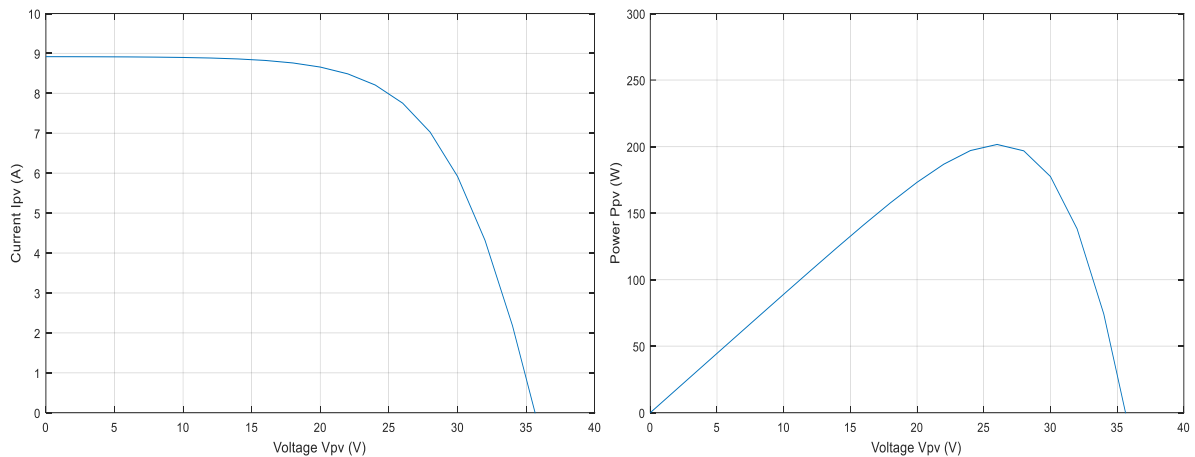


**Figure III- 13: I(V) and P(V) characteristics of a Six-parameter cell model.**

The characteristic power-voltage of a solar cell in conditions of  $E=1000 \text{ W/m}^2$  and  $T=25^\circ\text{C}$ . The maximum power is  $P_{\text{max}} = 205\text{W}$ . It is noted that, when the voltage increases the power increases until it reaches the optimal value ( $P_{\text{max}}$ ) then it decreases.

### III.3.6. Simulation of Five -parameter Model

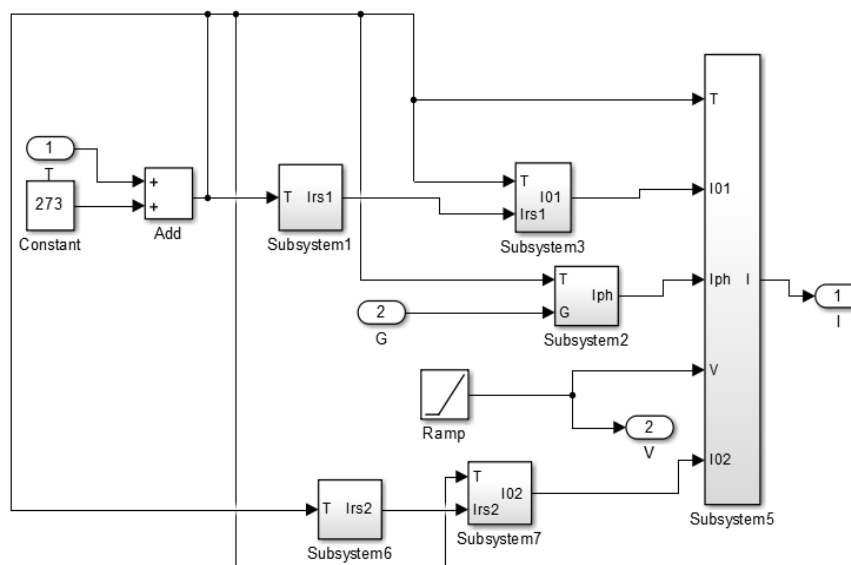


**Figure III- 14: schema of a current of Five -parameter Model.**

The results obtained from the simulation (programming using the MATLAB software) of a current characteristics -voltage I(V) and power-voltage P (V) of the photovoltaic cell In Five-parameter conditions ( $T = 25^\circ\text{C}$ .  $E = 1000 \text{ W} / \text{m}^2$ ) are represented in the following figure:

The following figure represents the current characteristic - voltage of a standard solar cell model in conditions of  $E = 1000\text{W} / \text{m}^2$  and  $T = 25^\circ\text{C}$ .

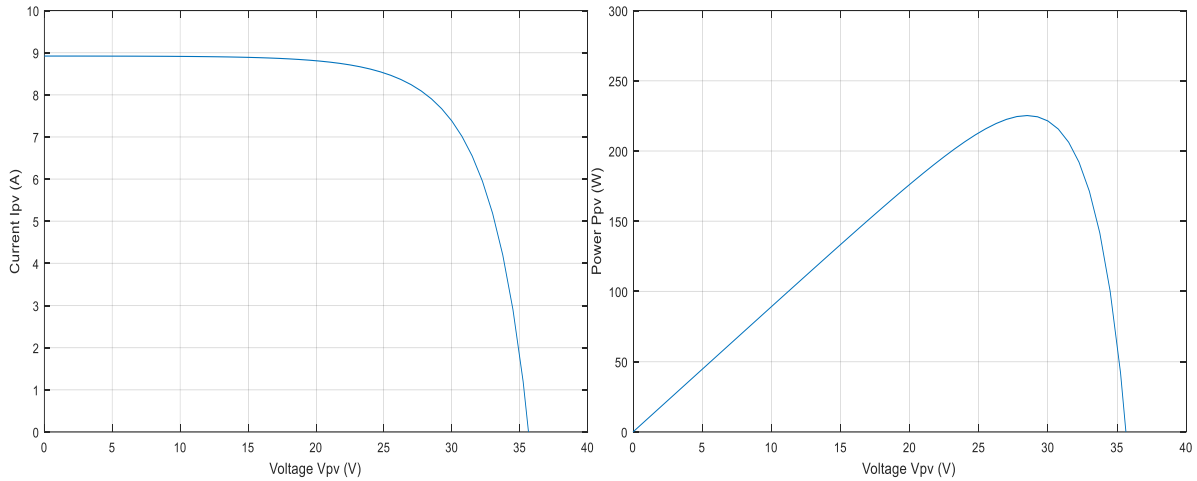


**Figure III- 15: I(V) and P(V) characteristics of a Five-parameter cell model.**

The characteristic power-voltage of a solar cell in conditions of  $E=1000 \text{ W/m}^2$  and  $T=25^\circ\text{C}$ . The maximum power is  $P_{\text{max}} = 227\text{W}$ . It is noted that, when the voltage increases the power increases until it reaches the optimal value ( $P_{\text{max}}$ ) then it decreases.

**III.3.7. Simulation of Four-parameter Model**

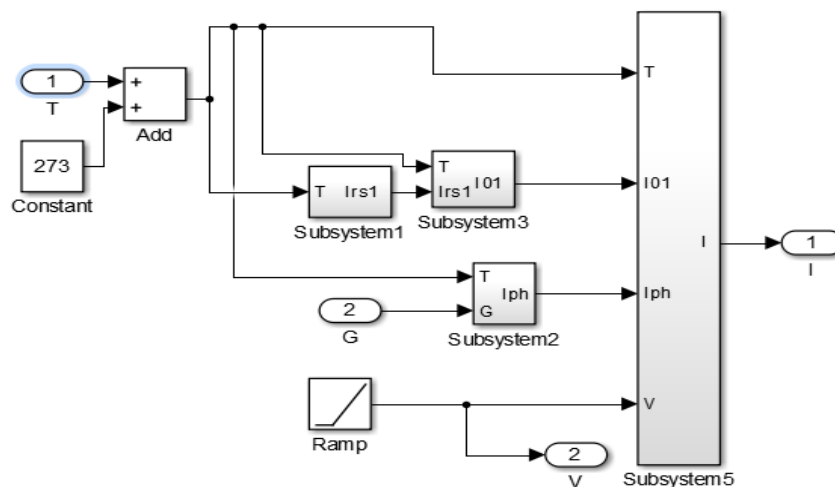


**Figure III- 16: schema of a current of Four-parameter Model.**

The results obtained from the simulation (programming using the MATLAB software) of a current characteristics -voltage I(V) and power-voltage P (V) of the photovoltaic cell In Four-parameter conditions ( $T = 25^\circ\text{C}$ .  $E = 1000 \text{ W} / \text{m}^2$ ) are represented in the following figure: The following figure represents the current characteristic - voltage of a standard solar cell model in conditions of  $E = 1000\text{W} / \text{m}^2$ and  $T = 25^\circ\text{C}$ .

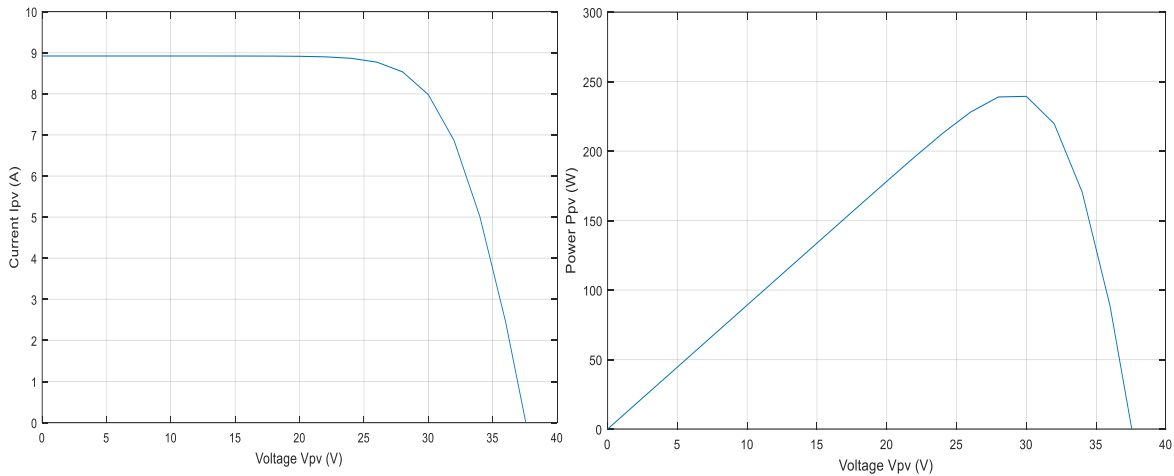


**Figure III- 17: I(V) and P(V) characteristic of a Four-parameter cell model.**

The following figure represents the characteristic power-voltage of a solar cell in conditions of  $E=1000 \text{ W/m}^2$  and  $T=25^\circ\text{C}$ . The maximum power is  $P_{\text{max}} = 243\text{W}$ . It is noted that, when the voltage increases the power increases until it reaches the optimal value ( $P_{\text{max}}$ ) then it decreases.

**III.3.8. Simulation of Three -parameter Model**

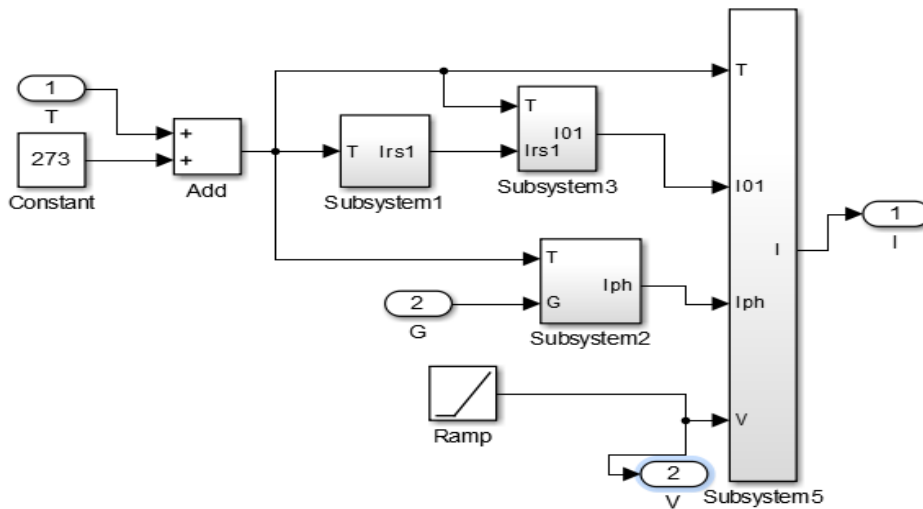


**Figure III- 18: schema of a current of Three -parameter Model.**

The results obtained from the simulation (programming using the MATLAB software) of a current characteristics -voltage I(V) and power-voltage P (V) of the photovoltaic cell In Three-parameter conditions ( $T = 25^\circ\text{C}$ .  $E = 1000 \text{ W} / \text{m}^2$ ) are represented in the following figure: The following figure represents the current characteristic - voltage of a standard solar cell model in conditions of  $E = 1000\text{W} / \text{m}^2$  and  $T = 25^\circ\text{C}$ .

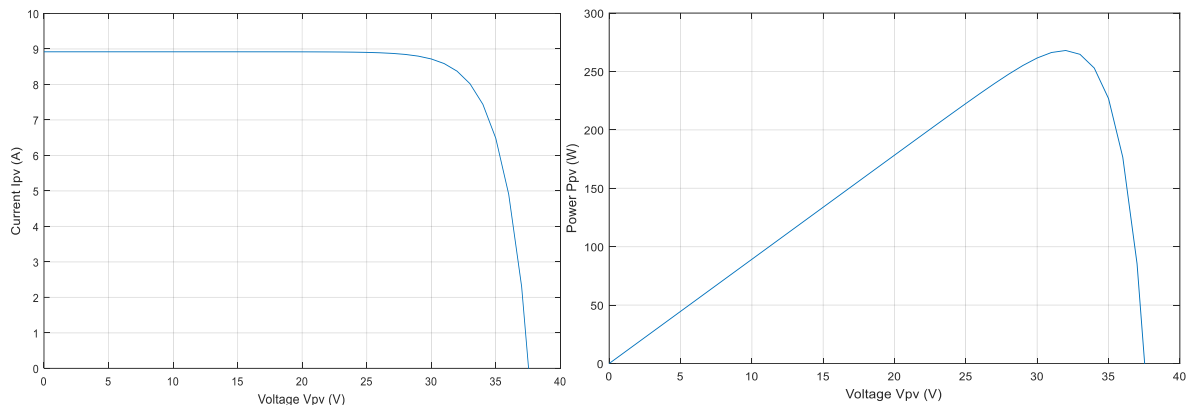


**Figure III- 19 :I(V) and P(V) characteristic of a Three-parameter cell model.**

The characteristic power-voltage of a solar cell in conditions of  $E=1000 \text{ W/m}^2$  and  $T=25^\circ\text{C}$ . The maximum power is  $P_{\text{max}} = 270\text{W}$ . It is noted that, when the voltage increases the power increases until it reaches the optimal value ( $P_{\text{max}}$ ) then it decreases.

### III.3.9. Simulation of based on technical and meteorological parameters Model

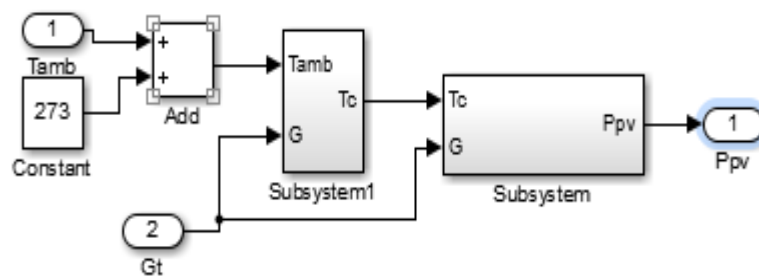


**Figure III- 20: schema of a power of based on technical and meteorological parameters Model.**

The results obtained from the simulation (MATLAB programming) of P energy properties of the PV are a based on technical and meteorological parameters model in conditions for solar radiation and heat on 04-06-2023 from 6 a.m. to 20 p.m In the new el hadjira touggourt . in the following form:

The following figure represents energy characteristic of the Simplified solar cell model. The maximum power is  $P_{\text{max}}=225\text{W}$ . It is noted that, when time increases power increases until it reaches the optimal value ( $P_{\text{max}}$ ) then it decreases. With an observation of a device malfunction at 15.30 p.m.

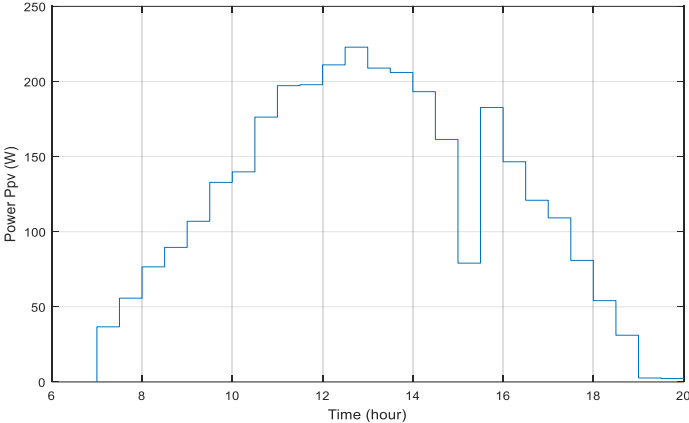


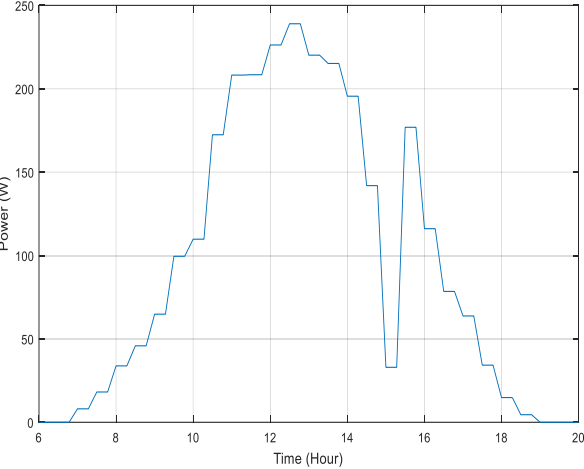
**Figure III- 21: P characteristic of a based on technical and meteorological parameters cell model.**

**III.3.10. Comparison between pv model**

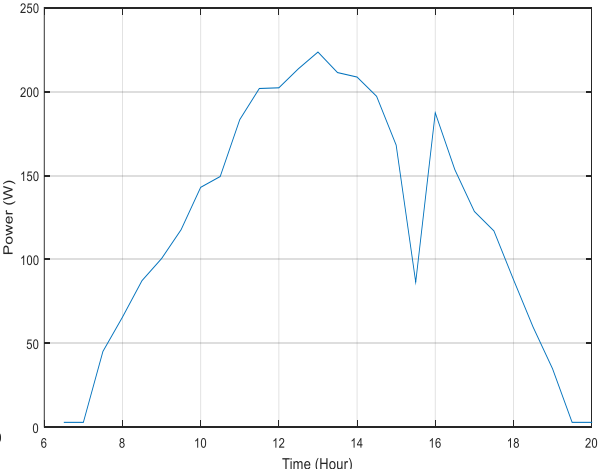
The following comparison is between nine models where we're going to compare the power between the different nine models by taking 04-06-2023 as a reference to change temperature and solar radiation from 6 a.m. to 20 p.m.

Our work will involve determining which nine models most closely resembles the model Yingli energy (YL250P\_29b), which states that the maximum peak power in 25 degrees and 1,000 W/m2 solar radiation is equal to 250W. This information is already available in Table II.1

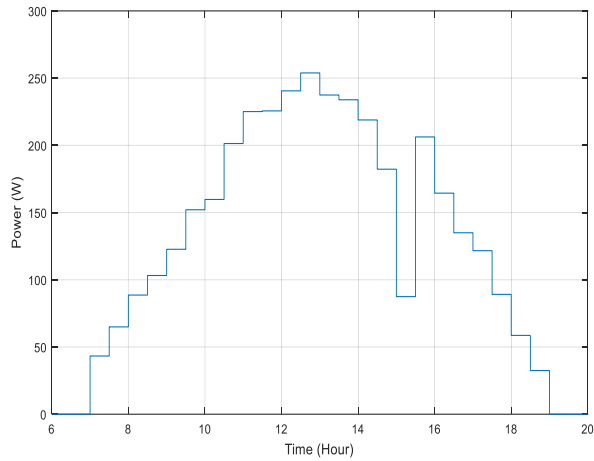
The following are the results of nine models simulations in Matalab for the day of 04-06-2023.



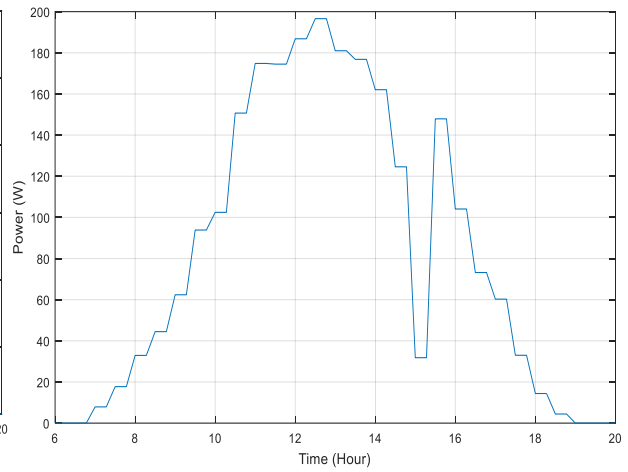
(a) Power changes for a standard model



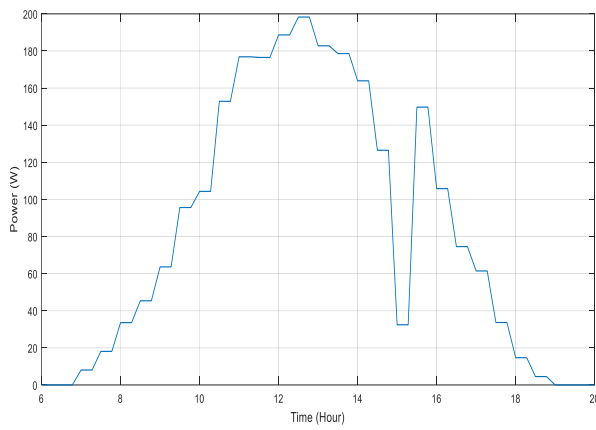
(b) Power changes for a simplified model



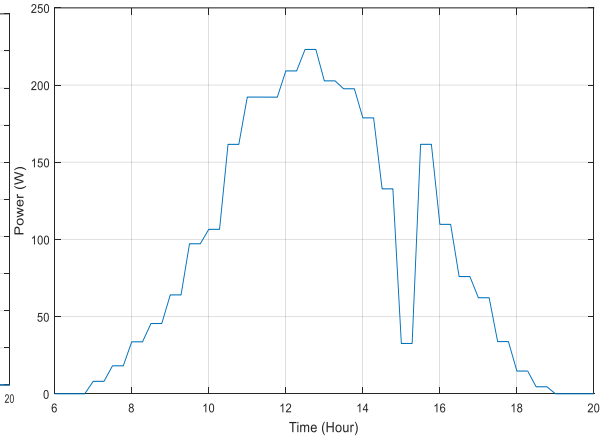
(c) Power changes for a based on solar irradiation model



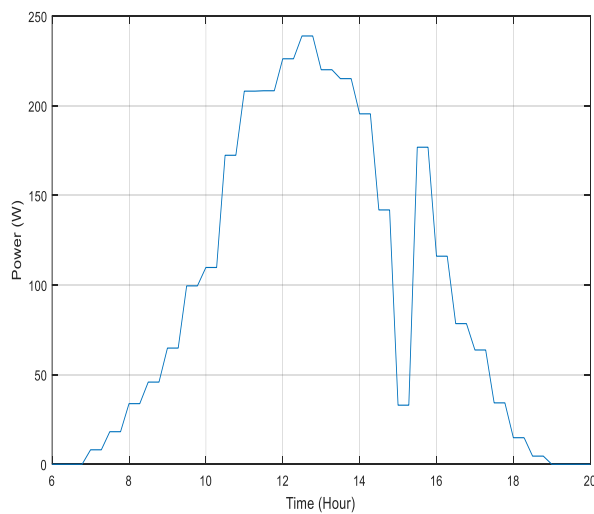
(d) Power changes for a Seven-parameter model



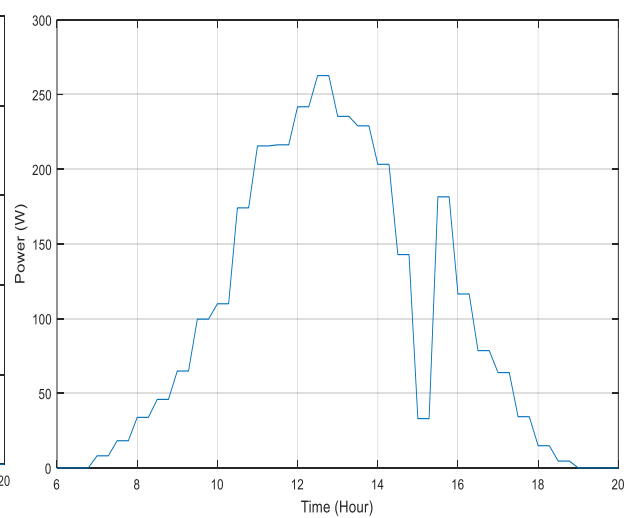
(e) Power changes for a Six-parameter model



(f) Power changes for a five-parameter model

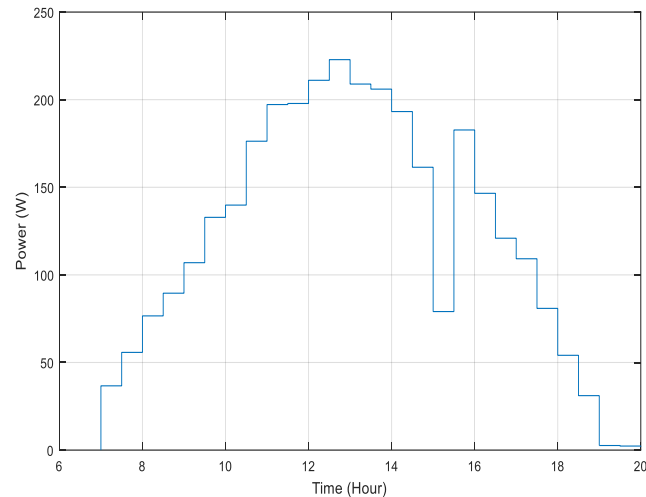


(G) Power changes for a four-parameter model



(H) Power changes for a three-parameter model





(I)Power changes for a based on technical and meteorological parameters model

**Figure III- 22: Results of the simulation of the nine models of the solar panel 1**

Note that the model based on solar irradiation is the closest and best simulation model in Matlab that offers us a similar force to Yingli energy (YL250P\_29b) manufacturing data based on solar radiation data taken from southern Algeria (el hedjira) where its maximum strength is equal to 254W at 12:30 and a solar radiation estimated at 1036 w/m<sup>2</sup>, which is the closest to 250W on manufacturing data as stated in Table II.1.

### III.3.11. simulation of inverter

We will choose in this work the three-phase inverter ordered by MLI

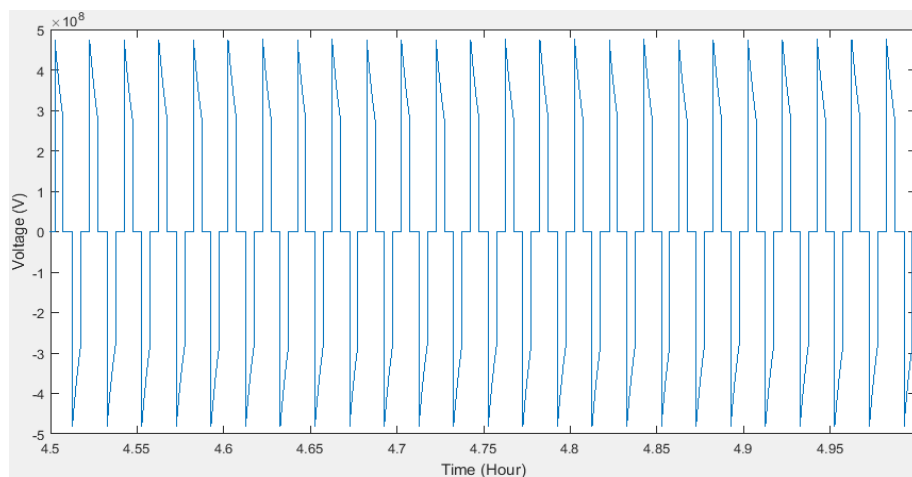


**Figure III- 23: Voltage (Va) output signal of the inverter.**

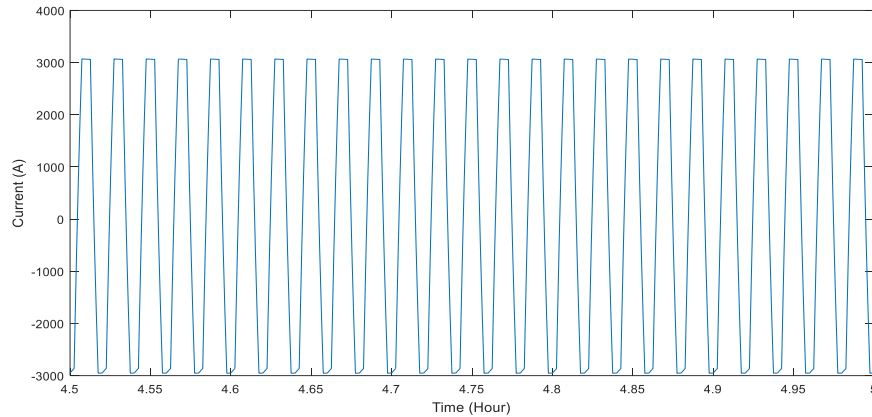


**Figure III- 24: current (Ia) output signal of the inverter.**

We simulated the inverter in the matlab environment, and then we got a rotational effort and current with some of the disturbances that Filter Lc will fill with the basic inverter simulation and must convert from DC to AC.

**III.4. validation of Photovoltaic System models**

In this part, we simulated the electrical generator station in the el hedjira area that produces 30MW in Matalab.

- We've been working on changing the models of the pv panels used at the station using the same manufacturing data.

- Station 30MW uses 120,000 Yingli energy panels (YL250P\_29b) divided into 30 fields with each field containing 4000 pv panels. There are 22 sequenced panels with one inverter with 1 MW capacity to convert the current from continuous to rotating with 30 inverter.

- The figures shapes show the results of the simulation.

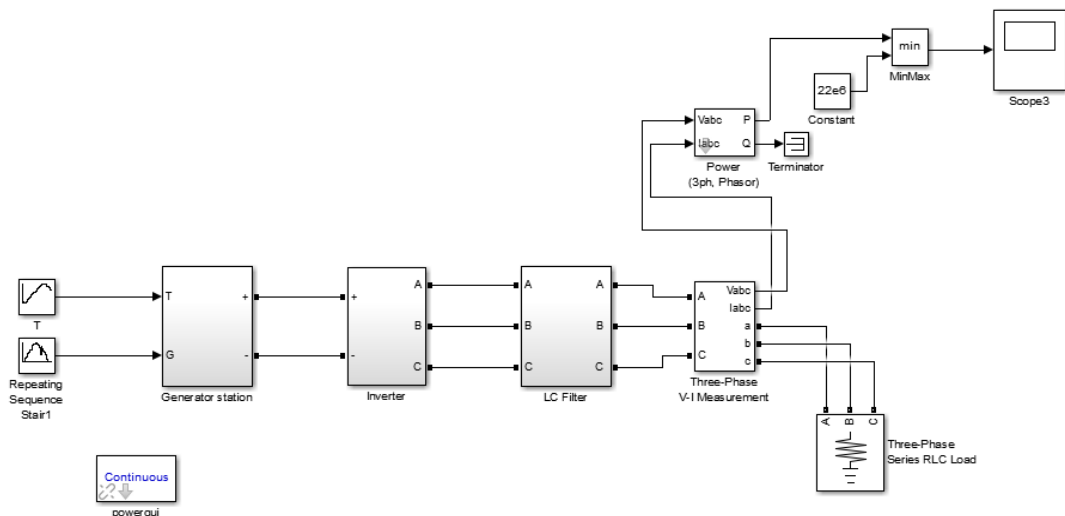
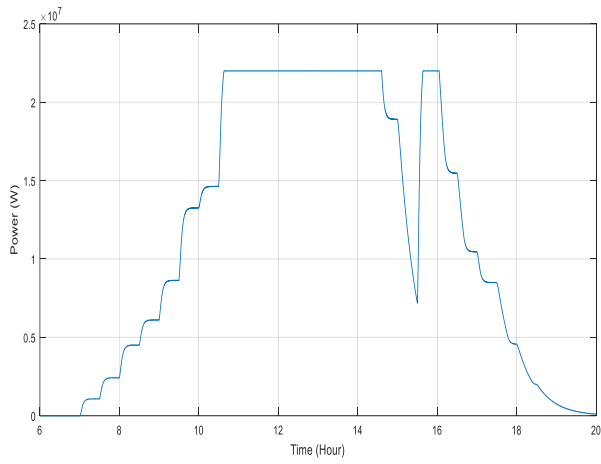
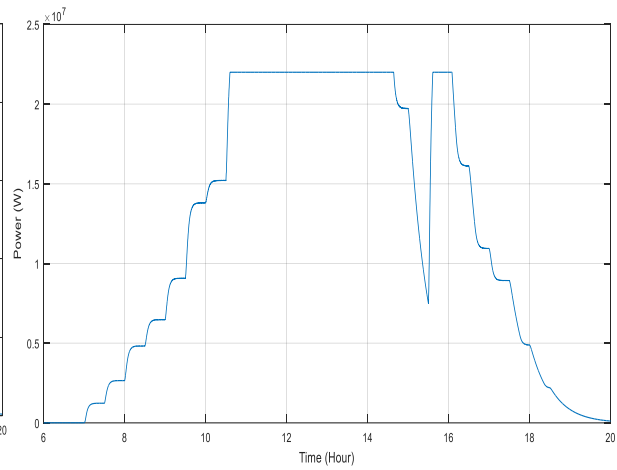


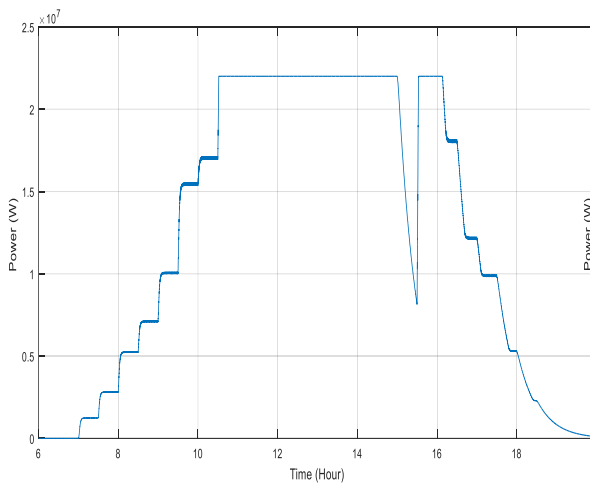
**Figure III- 25: The simulation of the PV generator station in Matalab.**



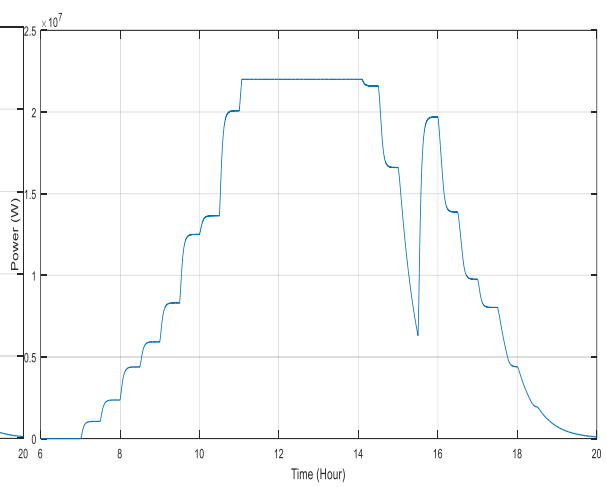
(a) Power changes for a standard model



(b) Power changes for a simplified model



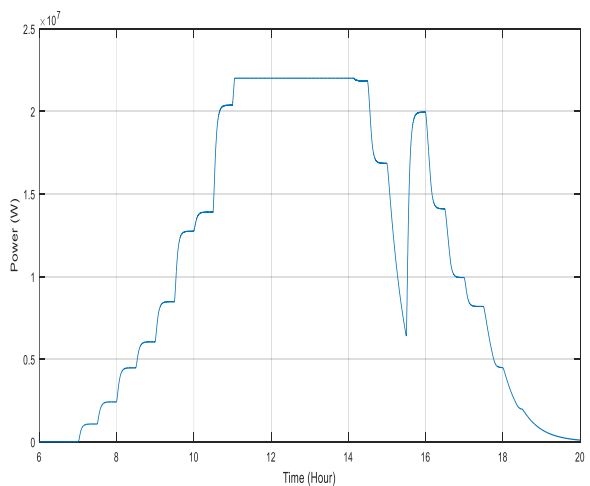
(c) Power changes for a based on solar



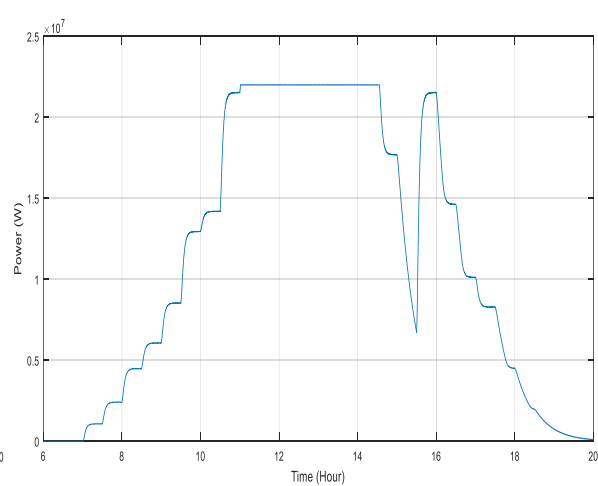
(d) Power changes for a Seven-parameter

irradiation model

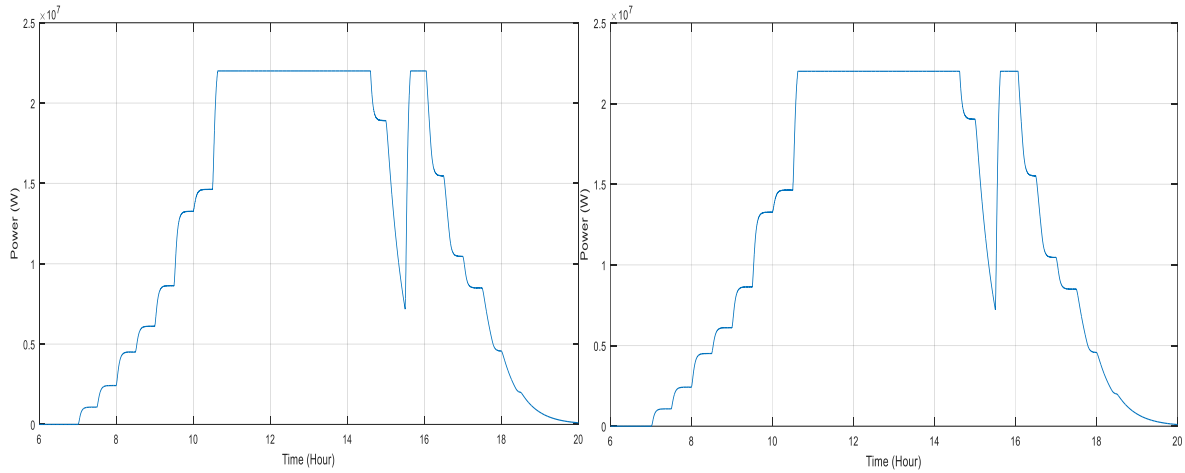
model



(e) Power changes for a Six-parameter model

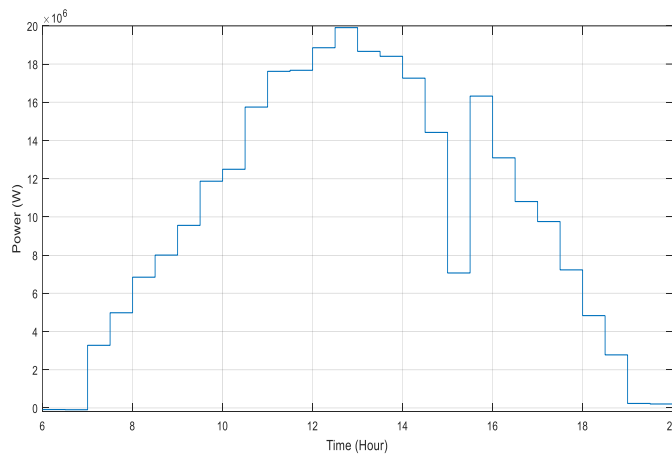


(f) Power changes for a five-parameter model



(G)Power changes for a four-parameter model

(H)Power changes for a three-parameter model



(I)Power changes for a based on technical and meteorological parameters model

**Figure III- 26 :Results of the simulation of the nine models of el-Hedjira station.**

The following figure shows the production of the day of 04-06-2023 at the el-Hedjira station

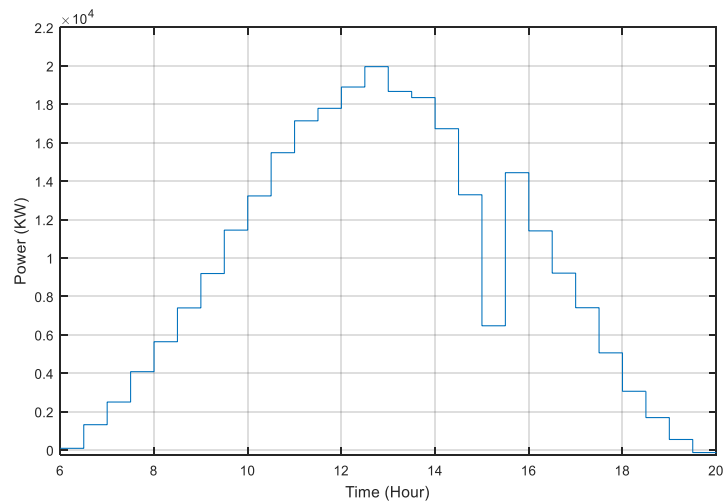


**Figure III- 27 :Production at the el-Hedjira station 2023-06-04.**

We note that the nearest model that can be rewarded for the production results of the el-Hedjira station is based on technical and meteorological parameters that depend on temperature and solar radiation changes as well as cable and inverter efficiency.

**Table (III.1): validation of Photovoltaic System models**

Model Time (Hour)	Power (MW)									
	Standard	Simplified	based on solar irradiation	2M7P	2M6P	2M5P	L4P	L3P	based on technical and meteorological parameters	Production at the el-Hedjira station
6:00-6:30	0	0	0	0	0	0	0	0	-0.2	0.1
8:00-8:30	4.5	4.8	6	3.5	4.3	4.3	4.6	4.7	7	5.8
10:00-10:30	14.6	153	17.5	14	14.3	14.8	14.8	14.8	12.5	13
12:00-12:30	22	22	22	22	22	22	22	22	19	19
14:00-14:30	22	22	22	21.5	21.5	22	22	22	17.5	17
16:00-16:30	(22_16)	(22_17)	(22_18)	(2_14)	(2_14.3)	(22_16.5)	(22_16.5)	(22_17)	13	11.8
18:00-18:30	(4.5_2.5)	(5_2.7)	(6_33)	(4_2)	(4_2.5)	(4.8_2.5)	(4.8_2.5)	(4.7_2.5)	5	3.8
19:00-20:00	(0.8_0)	(0.8_0)	(8_0)	(0.7_0)	(0.7_0)	(0.8_0)	(0.8_0)	(0.8_0)	0.2	-0.1

### III.5. Conclusion

After we simulated each of the components of the PV system, which eventually enabled us to simulate the entire system according to the models of the PV generator to get the results of the force that revealed to us that a model based on technical and meteorological parameters is the best model that can be used in southern Algeria, And the model based on solar irradiation is the best in production when using a single panel , and the results have shown that the Four-parameter model is the best in I(V) and P (V) characteristic.

## **General conclusion**

With their lack of greenhouse gas emissions, waste production, and overall environmental friendliness, renewable energy sources are a great replacement for fossil fuels. They never run out and enable decentralized manufacturing that is tailored to the demands of the region and the available resources. They also provide a great deal of energy independence.

Out of all the renewable energy sources, photovoltaic energy has attracted the greatest attention and development. This is because of its significant cost reduction, huge global solar potential, and efficiency improvements.

An in-depth bibliographical research has enabled us to obtain several models of PV panels discovered in previous years.

The work presented in this Thesis related to the study of the performance of the PV system when the PV models differ, especially in southern Algeria. This work is therefore divided into two sections. The first section relates to the different nine models and the results of the force they provide when applied to only one panel. The second section presents the application of the different nine models at a generator station containing 120,000 panels and their verification by comparing them with realistic results.

The main findings showed that the best model that can be relied upon when only one panel is produced is one based on solar irradiation, but the best reliable model for a large generator station in southern Algeria is one based on technical and meteorological parameters.

- [1]. Rawat, R., Kaushik, S.C., Lamba, R., 2016. A review on modeling, design methodology and size optimization of photovoltaic based water pumping, standalone and grid connected system. *Renew. Sustain. Energy Rev.* 57, 1506–1519.  
<https://doi.org/10.1016/j.rser.2015.12.228>
- [2]. Sampaio, P.G.V., González, M.O.A., 2017a. Photovoltaic solar energy: Conceptual framework. *Renew. Sustain. Energy Rev.* 74, 590–601.  
<https://doi.org/10.1016/j.rser.2017.02.081>
- [3]. Ibrahim, I.A., Khatib, T., Mohamed, A., 2017. Optimal sizing of a standalone photovoltaic system for remote housing electrification using numerical algorithm and improved system models. *Energy* 126, 392–403. <https://doi.org/10.1016/j.energy.2017.03.053>
- [4]. Boughali, S., Benmoussa, H., Bouchekima, B., Mennouche, D., Bouguettaia, H., Bechki, D., 2009. Crop drying by indirect active hybrid solar - Electrical dryer in the eastern Algerian Septentrional Sahara. *Sol. Energy* 83, 2223–2232.  
<https://doi.org/10.1016/j.solener.2009.09.006>
- [5]. abada Z. "Political, economic and social aspects of renewable energies". Course University of Kasdi Merbah – Ouargla. 2023/2024.
- [6]. Khezzar R, Zereg M, Khozzar A. Comparison of different electrical models and determination of the characteristic IV parameters of a photovoltaic module. *Journal of Renewable Energies.* 2010;13(3):379–88–88.
- [7]. Iaggoune M.L., Serraye M. "Technical and economic study of a photovoltaic installation". Memory of master academic University of Kasdi Merbah – Ouargla. 12/06/2022.
- [8]. Dida M. "Study and improvement of photovoltaic conversion systems in arid and semi-arid areas". Memory of Doctorate 3rd cycle University of Kasdi Merbah – Ouargla. 16/12/2021.
- [9]. Hananou F, Rouabah A. "Modelling and simulation of a photovoltaic system". Memory of master academic University of Kasdi Merbah – Ouargla. 09/06/2014.
- [10]. Boxwell, M. (2012). *Solar Electricity Handbook: A Simple, Practical Guide to Solar Energy : how to Design and Install Photovoltaic Solar Electric Systems.* United Kingdom: Greenstream Publishing.
- [11]. Goetzberger, A., Hoffmann, V.U. (2005). *Photovoltaic Solar Energy Generation.* Germany: Physica-Verlag.
- [12]. ]. abada Z. "Integration of renewable resources into electricity networks". Course University of Kasdi Merbah – Ouargla. 2023/2024.
- [13]. Negin M, Mokhtar B. A review of the application of photovoltaic panels in water desalination. *Materials Chemistry and Mechanics.* 2023;1(3):8-15.
- [14]. *Membrane and Desalination Technologies.*(2010).Germany: Humana Press.

- [15]. Torres J, Vivar M, Fuentes M, Palacios AM. SolWat technology for simultaneous wastewater disinfection and higher energy generation utilizing PV module front surface. *Journal of Water Process Engineering*. 2024;57:104698.
- [16]. Photovoltaic solar energy conversion : technologies applications and environmental impacts. (2020). Academic Press.
- [17]. BECHERIF B, AILAS G. "Study and simulation of a one-phase photovoltaic power generation system not connected to the grid" Memory of master University of Abubakr Belkaid– Tlemcen. 29 / 06 / 2022.
- [18]. Changmai P, Nayak SK, Metya SK. Estimation of PV module parameters from the manufacturer's datasheet for MPP estimation. *IET Renewable Power Generation*. 2020;14(11):1988-96.
- [19]. K. Yu, J. J. Liang, B. Y. Qu, X. Chen, and H. Wang, "Parameters identification of photovoltaic models using an improved JAYA optimization algorithm," *Energy Convers. Manage.*, vol. 150, pp. 742\_753, Oct. 2017, doi: [10.1016/j.enconman.2017.08.063](https://doi.org/10.1016/j.enconman.2017.08.063).
- [20]. L. L. Jiang, D. L. Maskell, and J. C. Patra, "Parameter estimation of solar cells and modules using an improved adaptive differential evolution algorithm," *Appl. Energy*, vol. 112, pp. 185\_193, Dec. 2013, doi: [10.1016/j.apenergy.2013.06.004](https://doi.org/10.1016/j.apenergy.2013.06.004).
- [21]. A. Askarzadeh and A. Rezaadeh, "Artificial bee swarm optimization algorithm for parameters identification of solar cell models," *Appl. Energy*, vol. 102, pp. 943\_949, Feb. 2013, doi: [10.1016/j.apenergy.2012.09.052](https://doi.org/10.1016/j.apenergy.2012.09.052).
- [22]. Q. Niu, L. Zhang, and K. Li, "A biogeography-based optimization algorithm with mutation strategies for model parameter estimation of solar and fuel cells," *Energy Convers. Manage.*, vol. 86, pp. 1173\_1185, Oct. 2014, doi: [10.1016/j.enconman.2014.06.026](https://doi.org/10.1016/j.enconman.2014.06.026).
- [23]. A. Omar, H. M. Hasanien, M. A. Elgendy, and M. A. L. Badr, "Identification of the photovoltaic model parameters using the crow search algorithm," *J. Eng.*, vol. 2017, no. 13, pp. 1570\_1575, 2017, doi: [10.1049/joe.2017.0595](https://doi.org/10.1049/joe.2017.0595).
- [24]. L. Wu, Z. Chen, C. Long, S. Cheng, P. Lin, Y. Chen, and H. Chen, "Parameter extraction of photovoltaic models from measured I-V characteristics curves using a hybrid trust-region reflective algorithm," *Appl. Energy*, vol. 232, pp. 36\_53, Dec. 2018, doi: [10.1016/j.apenergy.2018.09.161](https://doi.org/10.1016/j.apenergy.2018.09.161).
- [25]. F. Bonanno, G. Capizzi, G. Graditi, C. Napoli, and G. M. Tina, "A radial basis function neural network based approach for the electrical characteristics estimation of a photovoltaic module," *Appl. Energy*, vol. 97, pp. 956\_961, Sep. 2012, doi: [10.1016/j.apenergy.2011.12.085](https://doi.org/10.1016/j.apenergy.2011.12.085).
- [26]. Z. Wei, C. Huang, X. Wang, and H. Zhang, "Parameters identification of photovoltaic models using a novel algorithm inspired from nuclear reaction," in *Proc. IEEE Congr. Evol. Comput. (CEC)*, Jun. 2019, doi: [10.1109/CEC.2019.8790223](https://doi.org/10.1109/CEC.2019.8790223).
- [27]. F. Almonacid, E. F. Fernández, T. K. Mallick, and P. J. Pérez-Higueras, "High concentrator photovoltaic module simulation by neuronal networks using spectrally corrected direct normal irradiance and cell temperature," *Energy*, vol. 84, pp. 336\_343, May 2015, doi: [10.1016/j.energy.2015.02.105](https://doi.org/10.1016/j.energy.2015.02.105).



---

## REFERENCES

---

- [28]. Ammari CH. "conversion photovoltaic ". Course University of Kasdi Merbah – Ouargla. 2022/2023.
- [29]. Lounis Y. "étude et simulation d'un convertisseur électrique interconnecté au réseau conventionnel" Memory of master academic University of universite mouloud mammeri, tizi-ouzou. 2015/2016
- [30]. Web site : <https://www.croatiaweek.com>. html .
- [31]. Web site : <https://hackaday.io/realsolarcars>. html .
- [32]. Web site : <https://akhbarak.net/news>. html .
- [33]. Web site : <https://fr.aliexpress.com>. html .
- [34]. Web site : <https://www.en.bio.aau.dk>. html .
- [35]. Web site : <https://www.lifestreamwater.com>. html .

### Abstract

The work presented in these presentations offers an experimental study of nine different models and their way in southern Algeria, after simulating them in Matalab, we found in the first place that at the performance of only one panel, the model based on solar irradiation is the best, and when a large station is set up, the performance of a model based on technical and meteorological parameters is the best.

**Key words:** PV system. PV modelling, simulation and verification of the PV system.

### Résumé

Le travail présenté dans ces présentations offre une étude expérimentale de neuf modèles différents et leur façon dans le sud de l'Algérie, après les avoir simulés à Matalab, nous avons constaté en premier lieu que, à la performance d'un seul panneau, le modèle basé sur l'irradiation solaire est le meilleur, et quand une grande station est mise en place, le rendement d'un modèle fondé sur les paramètres techniques et météorologiques est le mieux.

**Mots clés:** système PV. Modélisation, simulation et vérification du système PV.

### المخلص

العمل المقدم في هذه الاطروحة يقدم دراسة تجريبية لتسعة نماذج مختلفة وطرق ادائها في جنوب الجزائر، بعد محاكاة لها في Matalab، وجدنا في المقام الأول أن النموذج القائم على التشعيع الشمسي هو الأفضل عند أداء لوح واحد فقط، وعندما يتم إنشاء محطة كبيرة يكون أداء النموذج القائم على الاعدادات التقنية والأرصاد الجوية هو الأفضل. **الكلمات الدالة:** نظام كهروضوئي. نمذجة كهروضوئية. محاكاة هذا النظام والتحقق منه.